Lack of Impact of Ocean Alkalinization Enhancement in Coastal Heterotrophic Bacteria Communities of the Canary Region

Author
Laura Verdugo Ros

Academic course
2023 / 2024

Directed by
Dr. Nauzet Hernández Hernández
Dr. Javier Arístegui Ruiz

Dissertation required to obtain the MSc degree in Oceanography

Lack of Impact of Ocean Alkalinity Enhancement in Coastal Heterotrophic Bacteria Communities of the Canary Region

Trabajo de fin de título

para la obtención del título de Máster Universitario de Oceanografía por la Universidad de Las Palmas de Gran Canaria

Laura Verdugo Ros

Curso 2023/2024

Tutores:

Dr. Nauzet Hernández Hernández

Dr. Javier Arístegui Ruiz

Departamento de Biología. Facultad de Ciencias del Mar

Instituto de oceanografía y Cambio Global (IOCAG)

Grupo de Oceanografía Biológica (GOB)

Proyecto de investigación ligado, OceanNETs

En Las Palmas de gran Canaria, a día 20 de Noviembre 2024

Fdo. Laura Verdugo Ros *Fdo. Nauzet Hernández Hernández* *Fdo. Javier Arístegui Ruiz.*

INDEX

ABSTRACT

In contrast to acidification, Ocean Alkalinity Enhancement (OAE) entails the augmentation of bicarbonate ion concentration in the oceanic water column. This technology has the potential to serve as a Negative Emission Technology (NET) for the mitigation of climate change. In addition to enhancing long-term carbon storage, the OAE has the potential to counteract ocean acidification. However, it is possible that this process may also affect the availability of essential inorganic nutrients and dissolved organic carbon, which are crucial elements for bacterial growth and metabolism in the oceans. The objective of this study was to analyze the impact of ocean alkalinity enhancement on the evolution of bacterial communities, specifically high nucleic acid (HNA) and low nucleic acid (LNA) heterotrophic bacteria, as well as changes in dissolved organic carbon (DOC), dissolved organic nitrogen (DON), and their optical properties (CDOM), in response to different alkalinity concentration scenarios in the environment. To this end, a series of nine TA levels were established in a mesocosms experiment and maintained for 33 days. No TA effects were observed in either the HB abundances or community structure. Furthermore, the dynamics of dissolved organic matter were not impacted by TA or by increases in bacterial abundances. The lack of impact of HB on organic matter dynamics suggests that viral lysis could play an important role in enhancing the pool of DOC under OAE. However, this should be considered a preliminary hypothesis that requires further validation through additional studies.

1. INTRODUCTION

Climate change has a profound impact on marine ecosystems, threatening their well-being and stability (IPCC, 2014; 2019; 2022). About 26% of anthropogenic CO_2 emitted in the last seven decades have been taken up by the ocean leading to the disruption of the inorganic carbon chemistry (Friedlingstein et al., 2022; Boesch, Field, & Scavia, 2000; Orr et al., 2005). The main effect is a process known as ocean acidification (OA), caused by the absorption of excess atmospheric CO_2 by the oceans which mainly results in a decrease in both seawater pH and calcium carbonate saturation states (Ω) (Huo et al., 2013; Piontek et al., 2010; Hall-Spencer & Harvey, 2019; Rockström et al., 2009; Williamson & Turley, 2012). It adversely affects marine organisms with calcified structures, such as the coccolithophorids, by constraining their ability to produce calcium carbonate structures, (Hall-Spencer & Harvey, 2019; Feely & Doney, 2011; Fox et al., 2020) and interferes with critical ecological processes like primary production (Hernández-Hernández et al., 2018; Riebesell et al., 2007) and respiration (Filella et al., 2018; Spilling et al., 2016). Furthermore, as a consequence of the greenhouse effects, surface ocean is warming at a higher rate than deep ocean leading to a strengthening of water column stratification (Sallée et al., 2021; Smith et al., 2009) or favoring the occurrence of marine heat waves (Baroni et al., 2020; Field et al., 2000).

Mitigating the effects of climate change, however, is not an easy task. Indeed, both the Fifth and Sixth Assessment Report (AR5 and AR6) of the Intergovernmental Panel on Climate Change (IPCC) indicated that 87% of the scenarios in which temperature targets established by the Paris Agreement are achieved, require the implementation of Carbon Dioxide Removal technologies (CDR) (Burns & Corbett, 2020; IPCC, 2018; 2022). Ocean-based strategies for CDR focus on reducing the concentration of atmospheric CO_2 as well as mitigating the adverse effects produced by its excess (Haszeldine et al., 2018; IPCC, 2018, 2022; Renforth et al., 2013). Some of the benefits associated with the CDR include compensate for past emissions, achieve carbon neutrality, stabilize the climate, and create effective carbon sinks. Since it is a novel field of study, the first challenges faced by these techniques include technical variability and scale impact, economic and financial terms, environmental and social impacts, uncertainty regarding effectiveness, and lack of governing regulations (Haszeldine et al., 2018; Gattuso et al., 2018, 2021).

Ocean Alkalinity Enhancement (OAE) is a type of CDR, specifically, a geoengineering that seeks to increase the capacity of the oceans to remove atmospheric CO_2 by accelerating a natural process, the mineral weathering. It involves a controlled addition of alkaline substances which enhance the formation of carbonate and bicarbonate ion species. Thus, dissolved CO_2 concentrations are reduced promoting the uptake of atmospheric CO_2 (Kheshgi, 1995; Feng et al., 2017; Harvey, 2008). Through this reaction seawater stores CO_2 in the form of carbonates, increasing its regulatory capacity. Modeling studies indicate that OAE could potentially remove between 3 to 10 Gt of atmospheric CO_2 per year (Feng et al., 2017; Harvey, 2008). It is important to note, however, that all model simulations are based on several assumptions that are not yet fully understood. (Hartmann et al., 2023; Kheshgi, 1995). Despite capturing CO_2 through OAE seems to have exciting potential, its feasibility depends on its scalability and on its environmental safety. However, it has significant limitations such as high energy consumption, high costs, the complexity of ocean-atmosphere interactions, and, ultimately, unknown environmental impacts (Harvey, 2008; Kheshgi, 1995). Extensive research on their feasibility, limitations and potential harmful effects are then necessary for their proper implementation.

Recent studies have increasingly examined the impact of Ocean Alkalinity Enhancement (OAE) on primary producers and higher trophic levels (Marín-Samper et al. 2024, Ferderer, 2022; Paul, 2024; Subhas, 2022). However, the influence on heterotrophic bacteria and their role in biogeochemical cycles has received comparatively less attention. Studies have shown that an increase in ocean alkalinity can significantly stimulate bacterial growth, which can occur because of the availability of more favorable conditions for bacterial metabolism, such as higher alkalinity and pH levels (Tiago et al., 2004; Doney et al., 2009; Hornick et al., 2017; Dang, 2020; Gao et al., 2021). This increase in the growth rate can also affect the composition and diversity of heterotrophic bacterial communities (Tiago et al. 2004). Changes in the bacterial community composition may cause cascading effects on the functioning of the ecosystem and nutrient cycling, as well as an increase in alkalinity that could stimulate the capacity of heterotrophic bacterial biodegradation (Nzila and Musa, 2021). This could lead to these bacteria becoming more efficient in the decomposition of organic matter, thus promoting greater nutrient rotation and recycling within marine ecosystems (Ji et al., 2018). However, many uncertainties remain regarding to the specific mechanisms and consequences of this stimulation. Thus,

additional research is required to understand the impact of OAE on heterotrophic bacterial populations.

Here, we study the effect of OAE in heterotrophic bacteria populations and their relation to the organic matter using a mesocosm approach. We hypothesize that the introduction of alkaline agents to the ocean, may significantly influence the abundance and activity of heterotrophic bacteria, ultimately affecting the decomposition of organic matter and the circulation of nutrients in marine ecosystems. Furthermore, it is anticipated that bacterial communities will vary with differing alkalinity levels, thereby providing a more comprehensive understanding of the impact of alkalinity on bacterial dynamics and biogeochemical processes in marine environments.

2. DATA AND METHODS

2.1. Experiment set up, sampling, and maintenance

The KOSMOS Gran Canaria 2021 experiment was conducted at the pier of Taliarte, Gran Canaria (Canary Island) from September 14 to October 16, 2021 (Fig.1). Nine 8 m^3 mesocosms bags (M) were mounted on floating frames, anchored to the pier, and closed at the bottom using a conical sediment trap as described by Goldenberg et al., 2022, and Bach et al. (2019b) (Fig.1). The mesocosms were arranged in a pseudo-random order along the pier to avoid potential bias associated with their location. On September 10, the nine mesocosms were concurrently filled with pre-filtered seawater (pore size of 3 mm) pumped from outside of the harbor nearshore areas at depths ranging between 2 and 12 m using a peristaltic pump operating at a flow rate of 14 $m^3 \cdot h^{-1}$ (model KUNZ SPF60, Flexodamp FD-50). The seawater was evenly distributed using a digital flowmeter**.**

To examine the consequences of an increase in total alkalinity (TA), a series of nine stages were established in intervals of 300 $\mu mol \cdot L^{-1}$, ranging from 0 $\mu eq \cdot kg^{-1}$ of added alkalinity (OAE0) to 2400 $\mu eq \cdot kg^{-1}$ (OAE2400) (Table 1). This was accomplished by adding stock solutions of Na_2CO_3 and $NaHCO_3$ previously equilibrated with air to the mesocosms on experiment day 4 (17^{th} of September). Solutions were prepared by dissolving the corresponding salts in 22 kg of deionized water. Different amounts of the solutions were added to adjust the total alkalinity to the target levels listed in Table 1. Salinity was adjusted to 35 $g \cdot kg^{-1}$ in each mesocosm using NaCl. CTD and pH profiles were carried

out after the addition of alkalinity solution to ensure successful alkalinity adjustment in each mesocosm.

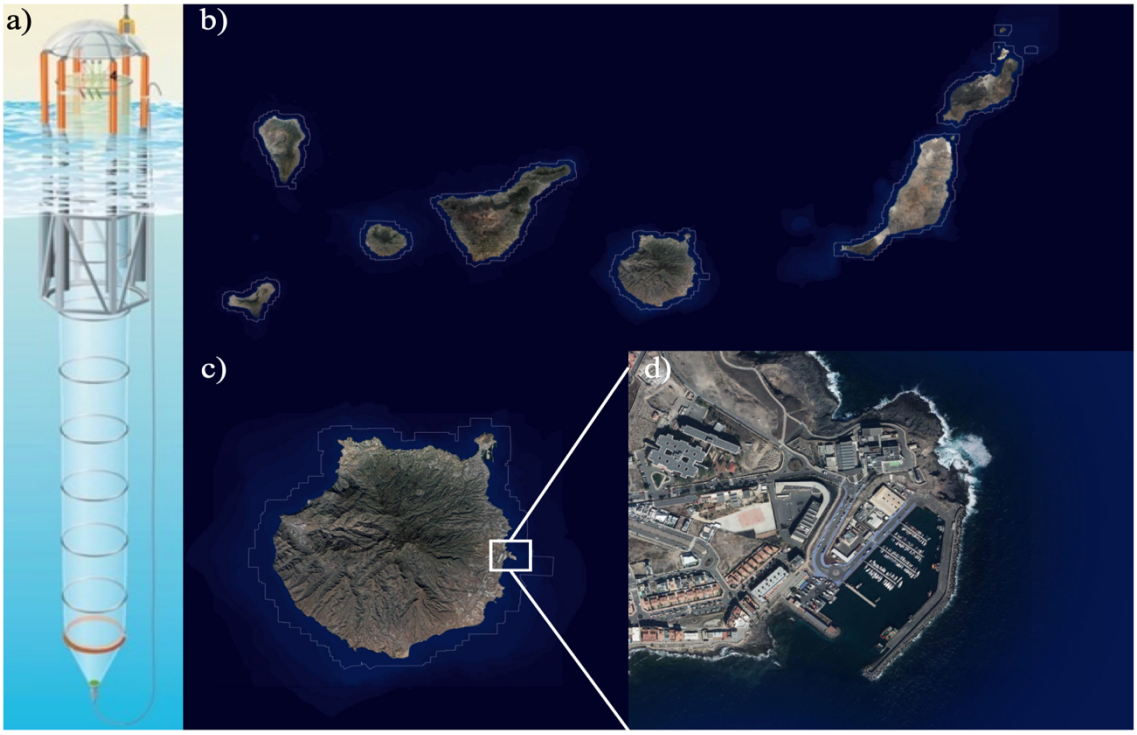

Figure 1. *(a) diagram of a mesocosm unit (extracted from Ferderer et al., 2022). (b) Geographical map of the Canary Islands.(c) Map of Gran Canaria indicating the location of Taliarte, where the experiment was conducted, as shown in figure d (Aviable at: https://visor.grafcan.es).*

Table 1. *Average values and standard errors of total alkalinity (TA), dissolved inorganic carbon (DIC), partial pressure of CO_2 (pCO_2), bicarbonate (HCO_3^-), and carbonate (CO_3^{2-}) ions, pH, and calcium carbon (Ω_{Ca}) and aragonite (Ω_{Ar}) saturation states from alkalinity manipulation on day 4 to the end of the experiment. Concentration units for TA, DIC, HCO_3^- and CO_3^2 are in $\mu mol \cdot L^{-1}$, for pCO_2 it is in µatm. First column, color code to be followed hereafter for each mesocosm (M). Second column, target TA increments.*

M	OAE	TA	DIC	pCO_2	HCO_3^-	CO_3^{2-}	pH	Ω_{Ca}	Ω_{Ar}
5	0	2427.7± 4.31	2119 ± 2.92	417.7 ± 2.87	1889.6 ± 2.59	219.4 ± 1.48	8.03 ± 0.003	5.2 ± 0.03	3.4 ± 0.02
1	300	2706.4 ± 10.24	2348.5 ± 3.27	435.6 ± 15.94	2078.6 ± 5.44	257.0 ± 6.02	8.06 ± 0.012	6.1 ± 0.14	4.0 ± 0.09
7	600	3003.7 ± 7.59	2593.6 ± 4.73	427.7 ± 6.34	2271.0 ± 5.60	310.0 ± 3.94	8.10 ± 0.006	7.3 ± 0.09	4.8 ± 0.06
4	900	3297.4 ± 4.45	2829.8 ± 4.53	429.8 ± 7.82	2456.2 ± 8.07	361.0 ± 4.49	8.14 ± 0.007	8.5 ± 0.11	5.6 ± 0.07
9	1200	3603.9 ± 7.27	3079.6 ± 4.95	438.2 ± 5.40	2654.1 ± 6.18	412.6 ± 4.03	8.16 ± 0.005	9.8 ± 0.09	6.4 ± 0.06
3	1500	3881.7 ± 8.23	3295.7± 6.65	435.2 ± 8.58	2814.8 ± 10.89	468.1 ± 6.55	8.19 ± 0.007	11.1 ± 0.15	7.3 ± 0.10
6	1800	4165.4 ± 7.77	3507.0± 6.43	429.7 ± 8.13	2969.3 ± 11.40	528.5 ± 6.92	8.22 ± 0.007	12.5 ± 0.16	8.2 ± 0.10
2	2100	4458.0 ± 7.42	3752.3± 6.72	443.7 ± 6.26	3160.9 ± 9.72	578.4 ± 5.21	8.23 ± 0.005	13.7 ± 0.12	9.0 ± 0.08
8	2400	4655.8 ± 22.09	3920.4± 13.53	461.7 ± 8.53	3299.0 ± 9.99	607.8 ± 9.15	8.23 ± 0.007	14.4 ± 0.22	9.4 ± 0.15

To obtain comprehensive depth-integrated samples, 2.50 m custom polypropylene tubes equipped with valves at both ends with an internal volume of 5L were employed. These tubes were used to collect samples every second day for over 33 days. Water samples were collected between 08:00 and 10:50 local time, then transferred into 10L plastic canisters, transported to the laboratories and sub-sampled. After sample collection, CTD profiles (CTD 60m, Sea and Sun Technology) were carried out from 0.50 to 3.00 m. The mesocosms were cleaned according to a specified protocol, both internally and externally. Sediment traps were cleaned using a funnel system to eliminate any biological growth along the walls and to minimize shading effects during the sampling period. Figure 2 provides a comprehensive summary of the daily activities conducted in the mesocosms. Further information about mesocosms maintenance may be consulted in Paul et al. (2024).

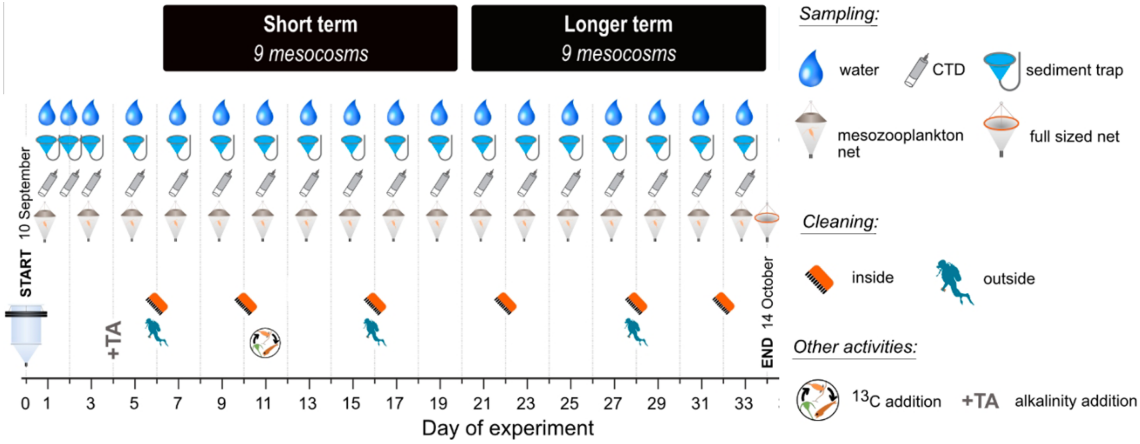

Figure 2. *Chronology of the activities carried out in the mesocosms during the experiment (extracted from Paul, et. al,2024).*

2.2. Measured variables

2.2.1. DIC

TA and dissolved inorganic carbon (DIC) samples were collected directly from custom samplers into 250 mL glass bottles ensuring they were filled with no air gaps to prevent contamination. These samples were then sterile filtered using 0.20 µm filters (SARSTEDT, Nümbrecht, Germany) with a peristaltic pump, taking care to keep the samples free of bubbles and minimize atmospheric contact. TA concentrations were determined via potentiometric titration using a Metrohm 862 Compact Titrosampler, with 0.05 M HCl as the titrant, an Aquatrode Plus (Pt1000), and a Unit 907 Titrando, following

the protocol described by Chen et al. (2022). The variation in TA measurements during the first three sampling days showed a maximum standard deviation of 6.50 µmol· kg^{-1}.

DIC concentrations were measured using an AIRICA system (Marianda, Kiel, Germany) equipped with a differential gas analyzer (LI-7000, LI-COR Biosciences GmbH, Bad Homburg, Germany). Measurements were conducted at room temperature over a 12-h period, as described by Gafar and Schulz (2018) and Taucher et al. (2017). The variability in DIC measurements during the initial sampling days had a maximum standard deviation of 10.20 µmol·kg^{-1}.

The values of TA and DIC were used to calculate other carbonate chemistry parameters such as pH, the partial pressure of CO_2 (pCO_2), the concentrations of bicarbonate (HCO_3^-), and carbonate (CO_3^{2-}) ions, and calcium carbon (Ω_{Ca}) and aragonite (Ω_{Ar}) saturation states using CO_2SYS v2.1 software (Lewis & Wallace, 1998). For these calculations, the carbonate dissociation constants (K1 and K2) according to Lueker et al. (2000), and the boron constant according to Uppström (1974) were used. The salinity was kept constant at 36.55 until day 17, when it was adjusted to 37.00 for the rest of the experiment.

2.2.2. Nutrients

Inorganic nutrients, nitrate (NO_3), nitrite (NO_2), phosphate (PO_4), and silicate (SiO_2), subsamples were collected in acid-cleaned polycarbonate bottles and filtered using 0.45 µm Sterivex filters (Merck). Subsequently, spectrophotometric analysis was conducted using an autoanalyzer system (QuAAtro autoanalyzer, SEAL Analytical) equipped with an autosampler (XY2 autosampler, SEAL Analytical) and a fluorescence detector (FP-202, JASCO), following the method described by Hansen and Koroleff (1999). Detection limits were determined daily and expressed as $\mu \pm 3\sigma$, corresponding to the concentration of the lowest standard in the calibration series. It's worth noting that deionized water was used for these measurements, which should not contain any detectable nutrients.

2.2.3. Chlorophyll a

500 mL subsamples were collected in dark bottles for Chla concentration measurements and filtered through 0.2 µm ø pore size (DHI GVS 20 µm, Hørsholm, Denmark, Whatman Nuclepore 2 µm and 0.2 µm, Maidstone, UK). Filters were then frozen at -20°C until analysis. For pigment extraction the filters were left submerged in 10 mL of acetone (90%) for 24 hours and at 4°C. The extract was subsequently analyzed on a fluorometer (Turner Design AU- 10, San Jose, USA) according to Welschmeyer (1994).

2.2.4. Dissolved Organic Matter

For the assessment of dissolved organic carbon (DOC) and total nitrogen (TN) measurements, 15 mL of water samples were filtered through GF/F filters, placed in high-density polyethylene bottles and stored frozen at -20°C until analysis. The samples were analyzed using a Shimadzu TOC-V analyzer. Before analysis, the samples were thawed, acidified with 50 mL of 50% H_3PO_4, and sparged with CO_2-free air for several minutes to remove the inorganic carbon. DOC and TN concentrations were determined based on the daily standard curves of potassium hydrogen phthalate (30–200 µM of C) and potassium nitrate (3-40 µM of N), respectively. DON was calculated as the difference between TN and the sum of nitrogenated inorganic nutrients (NO_3, NO_2, and NH_4). Deep-sea water reference material, containing 39–43 µM C, and 30-32 µM of N, provided by D. A. Hansell laboratory at the University of Miami, were analyzed daily.

2.2.5. Chromophoric Dissolved Organic Matter

Subsamples for chromophoric dissolved organic matter (CDOM) were collected in opaque 50 mL glass bottles. To obtain the absorbance spectra, a Jasco V-750 spectrophotometer in conjunction with a quartz cuvette of 10 cm of path length were used. Measurements were taken across a range of wavelengths (190 nm to 900 nm). Prior to each sample measurement, Milli-Q ultrapure water was used as a blank. The raw and blank spectra were first trimmed to 250–700 nm, the range where CDOM has higher absorbance and is more relevant for analysis. Blank spectra were then subtracted from the sample spectra for baseline correction. Afterward, the mean absorbance measured between 600 and 700 nm was subtracted from the entire spectrum to eliminate non-specific absorbance contributions or background noise. This process eliminated any background errors, ensuring that the measured absorbance uniquely represented CDOM. Once the data were processed, the absorbance was converted to absorption coefficient by means of the equation:

$$a_\lambda = 2.303 \cdot \frac{Abs_\lambda}{L}$$

Where Abs_λ is the absorbance at wavelength λ, L the path length of the cuvette (in meters), and 2.30 the factor converting decadic to natural logarithms. Within the spectra, absorbance at 254 nm and 325 nm were analyzed as proxies for DOC and CDOM concentration, respectively.

Spectral slopes were calculated from the natural logarithmic transformed absorption spectra within the ranges of 275-295 nm and 350-400 nm, according to the method of Helms et al. (2008). Their ratio (Sr) is highly sensitive to variations in the average molecular weight of the CDOM (Helms et al., 2008; 2013).

2.2.6. Heterotrophic bacteria

A FACScalibur flow cytometer (Becton and Dickinson) was used to count heterotrophic bacterial (HB) abundances. 1.60 mL samples were fixed with paraformaldehyde at a final concentration of 2%, refrigerated at 4°C for 30 min, and finally stored in liquid nitrogen until analysis. To identify HB, 400 µL subsamples were stained with the fluorochrome SYBR Green I (Molecular Probes) in a final dilution of 100x of the commercial product. The samples were run at a low flow rate of 16 $\mu L \cdot min^{-1}$. Yellow-green latex beads (Polysciences, Inc., Warrington, PA, USA) of 1 µm of diameter were added as an internal standard. HB were identified based on their distinct signatures of side scatter (SSC) versus green fluorescence (FL1) scatter plots.

2.3. Data analysis

To investigate the potential effects of OAE on heterotrophic community and organic matter dynamics throughout the experiment, Reduced Major Axis linear regressions (Sokal and Rohlf, 2013) between log-transformed LNA, HNA, HB, DOC, DON, a_{325}, a_{254}, S_r, and Chla, and TA were performed for each phase. For that purpose, data was averaged per mesocosm and phase. Due to the precipitation occurred in the highest treatment (M8) during the second phase, it was excluded from the statistics. The confidence level for all analysis was set at 90% ($p < 0.10$). Normality assumptions were checked using Q-Q plots and Shapiro-Wilk tests of the residuals. All statistical analyses were conducted in R Statistical Software (v4.1.2; R Core Team, 2021).

3. RESULTS

3.1. Treatment achievement and phase determination

The experiment involved the addition of TA in increments of 300 $\mu mol \cdot L^{-1}$, starting on day 4, and resulting in stable levels of DIC and TA until day 21. Afterwards, indirect abiotic precipitation occurred in the highest treatment, 2400 $\mu mol \cdot L^{-1}$ (M8). Visible precipitates formed on the mesocosm walls from day 28 toward the end of the experiment,

resulting in a loss of approximately 293.70 µmol·L^{-1} of TA and 175.30 µmol ·L^{-1} of DIC (Fig. 3a and b).

pH levels increased in accordance with the gradient applied, ranging from 8.03 in the control to nearly 8.30 in the highest treatment, and were maintained until day 17. Thereafter, no differences were observed among the three highest TA treatments (Fig. 3c). pCO_2, on the other hand, remained significantly unchanged among the mesocosms (444.82 ± 4.28) despite the TA gradient due to the balanced nature of the alkalinity manipulation (Fig. 3d). On day 17, pCO_2 levels began to decline to the end of experiment in all mesocosms except in M2 and M8, reaching values close to 402.98 ± 28.99. On day 21, pCO_2 concentration in M2 decreased drastically to match those in the rest of mesocosm. In contrast, M8 continued increasing reaching up to 432.65± 17.30 at the end of the experiment. This value was approximately 50 µatm higher than the other treatments from day 27 onwards, reaching approximately 100 µatm above ambient levels at the end of the experiment (Fig. 3c). As a result of the increase in pCO_2 in this treatment, pH levels decreased from 8.24 on day 18, to 8.16 on day 33 (Figs. 3c and d).

On the basis of carbon chemistry but also in the phytoplankton response observed by Marín-Samper et al. (2024), the experiment was divided into two phases. The period between days 5 and 19 was designated as phase I. It was characterized by a short-term stabilization period. On day 20, phase II began. It was marked by the abiotic precipitation occurred in M8, and a significant change in the biological response between mesocosms (Figs. 3a and b, and 4.d).

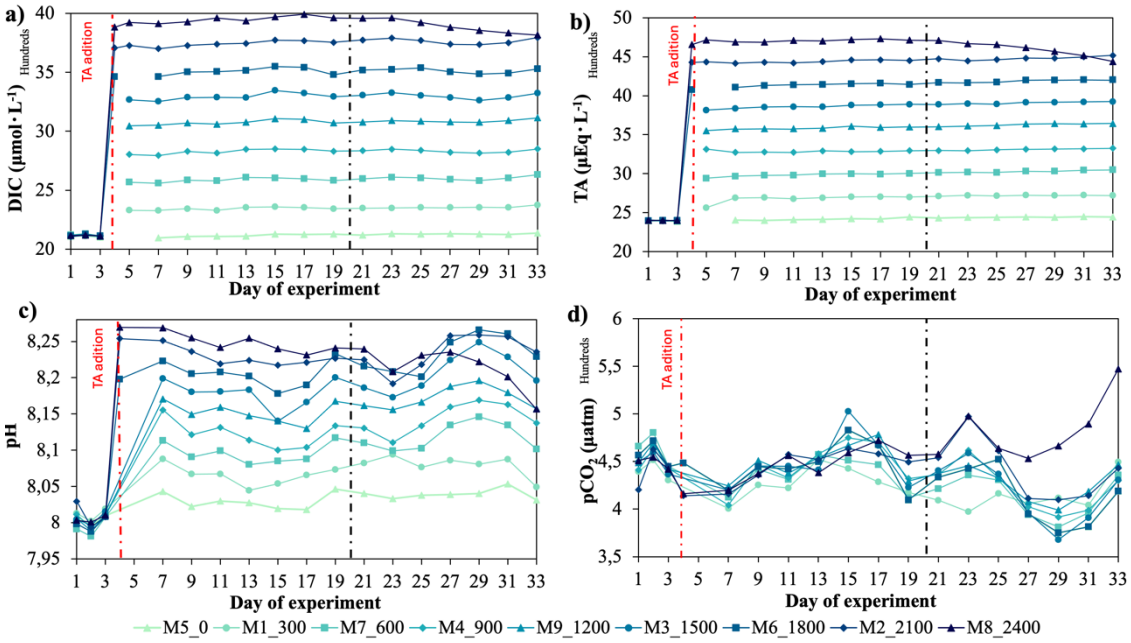

***Figure 3**. Temporal development of (a) dissolved inorganic carbon (DIC), (b) total alkalinity (TA), (c) pH (on a seawater scale) and (d) partial pressure of CO_2 (pCO_2) over the course of the experiment for each mesocosm. The x-axis represents the number of days that have passed since the beginning of the experiment. Vertical dashed red line indicates the day of TA manipulation and beginning of phase 1. Vertical dashed black line delimits first phase from second phase.*

3.2. Inorganic nutrients and phytoplankton response

PO_4 concentration before TA addition remained about 0.11 ± 0.01 µM. Following the addition of TA, a decline in PO_4 concentration was observed in the mesocosms, with average values decreasing from 0.11 ± 0.003 µM to 0.01 ± 0.004 µM on day 13 (Fig. 4a). No significant TA effects in PO_4 concentration were observed during this period (Fig. S1). From day 15 to 19, an increase in PO_4 concentration was observed preceding the beginning of the second phase. M7 exhibiting the highest increase from 0.05 to 0.09 µM. After these two significant fluctuations and throughout the phase II, phosphate concentration in all mesocosms stabilized around 0.05 ± 0.001µM.

A comparable decline in PO_4 concentration was observed in SiO_2 during Phase I, although in this instance, the concentration decreased until day 19. As the study progressed to the second phase, the differences in SiO_2 concentrations among the mesocosms became more pronounced, yet no TA effect was observed (Fig. S2). Two groups of mesocosms may be observed: the first, composed of M9, 3, and 1, presented relatively stable concentrations around 0.18 ± 0.04 µM, while the second, formed by the rest of mesocosms presented values around 0.29 ± 0.05 µM.

The concentrations of nitrate and nitrite (NO_x) were found to be exceedingly low, with some sampling days exhibiting values that fell below the limits of detection of the analytical technique employed. During the initial phase, a pronounced increase was observed on day 5, which may have been caused by contamination during the addition of TA. Additionally, a slight increase was observed between days 7 and 15. Subsequently, NO_x concentrations were undetectable until day 17. In the second phase, an initial slight increase was followed by stabilization of the concentrations towards the end of the sampling period. It should be noted that NO_x remained below 0.10 µM throughout the experiment. No TA effect was observed (Fig. S3).

As illustrated in Figure 4d, the concentration of Chla remained relatively low during the initial phase, oscillating between 0.04 and 0.33 $mg \cdot m^{-3}$. Chla concentrations did not exhibit neither significant variations in response to changes in nutrient levels nor differences among mesocosms, or TA effects (Table 2) during this period. However, in the second phase, an increase in Chla was observed between days 21 and 27, followed by a sharp decline after reaching the peak value, besides nutrient concentrations remained similar to those in the first phase. A statistically significant positive TA effect was observed in Chla in the second phase (Table 2).

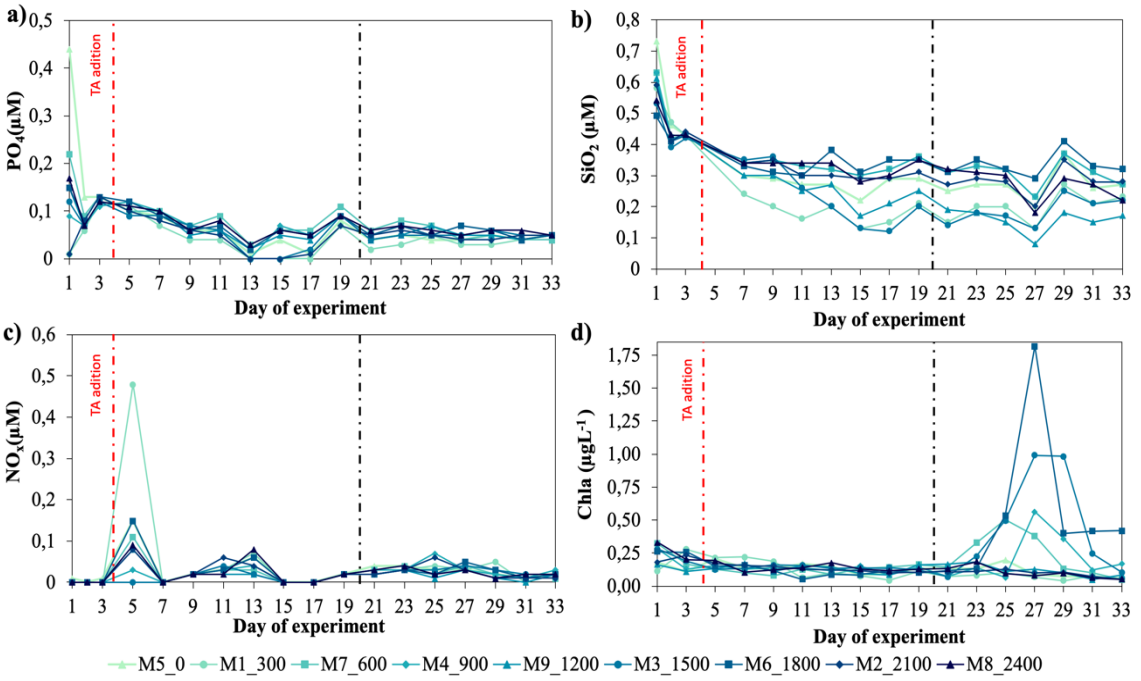

Figure 4*. Temporal development of (a) phosphate (PO_4), (b) silicate (SiO_2), (c) nitrate + nitrite (NO_x), and (d) chlorophyll a (Chla) over the course of the experiment for each mesocosm (M). The x-axis represents the number of days that have passed since the commencement of the experiment. Vertical dashed red line indicates the day of TA manipulation and beginning of phase 1. Vertical dashed black line delimits phase 1 from phase 2.*

3.3. Organic nutrients and its optical characteristics

The concentration of DOC exhibited a gradual increase across all mesocosms from the initiation of the experiment to its conclusion (Fig. 5a). The initial values (96.34 ± 1.51 µM) were consistent with those observed in coastal waters of the Canary region, reaching a maximum of 156.49 ± 2.39 µM on day 33. On day 21, there was a marked increase in DOC concentration, which coincided with an increase in Chla (Fig. 4c and fig. 5a). No TA effect was observed in either phase I or phase II (Table 2).

In contrast, DON exhibited a comparable trend to inorganic nutrients during the initial phase, initially declining from the outset of the experiment until day 13, before subsequently increasing at a gradual rate until day 27 (Figs. 4a-c and fig. 5b). On day 29, DON reached its highest concentration in the high treatments, coinciding with the decline of the bloom. Enhanced DON concentrations were rapidly removed from the water column, exhibiting values similar to those of the other mesocosms on day 31. The relationship between DON concentrations and Chla is corroborated by the positive TA effects observed in DON during the second phase, which align with the analogous effect observed in Chla (Table 2).

The C/N ratio of dissolved organic matter showed an increasing trend from 10.49 ± 0.82 on day 1 up to 17.19 ± 0.88 on day 11, after which the values stabilize around 16.91 ± 0.27 (Fig. 5.c). A negative and positive TA effect in phase I and II, respectively was observed in C/N (Fig. S7) coinciding with DON (Fig. S6).

a_{254}, as a proxy for DOC, showed a consistent relationship with DOC dynamics, showing a steady increase throughout most of the experimental period. In contrast to DOC, a significant negative effect of TA was observed in phase I (Table 2). From day 27, a_{254} increased sharply in all mesocosm except M8. This increase of a_{254} was uneven among the mesocosm showing significant differences yet these differences were not TA related (Table 2).

In a_{325}, during the first phase, a general decrease in absorbance was observed, followed by a slight upward trend from the start of the second phase, which continued until the end of the experiment. Between days 23 and 27, an increase was noted, with values rising from 0.22 ± 0.04 m^{-1} to 0.02 ± 0.05 m^{-1}.

Figure 6c shows that Sr concentrations remained stable during both phases of the experiment. However, between the end of the first phase and the beginning of the second (days 17 to 23), a notable increase in Sr levels was observed in M4, 9, 5 and 8.

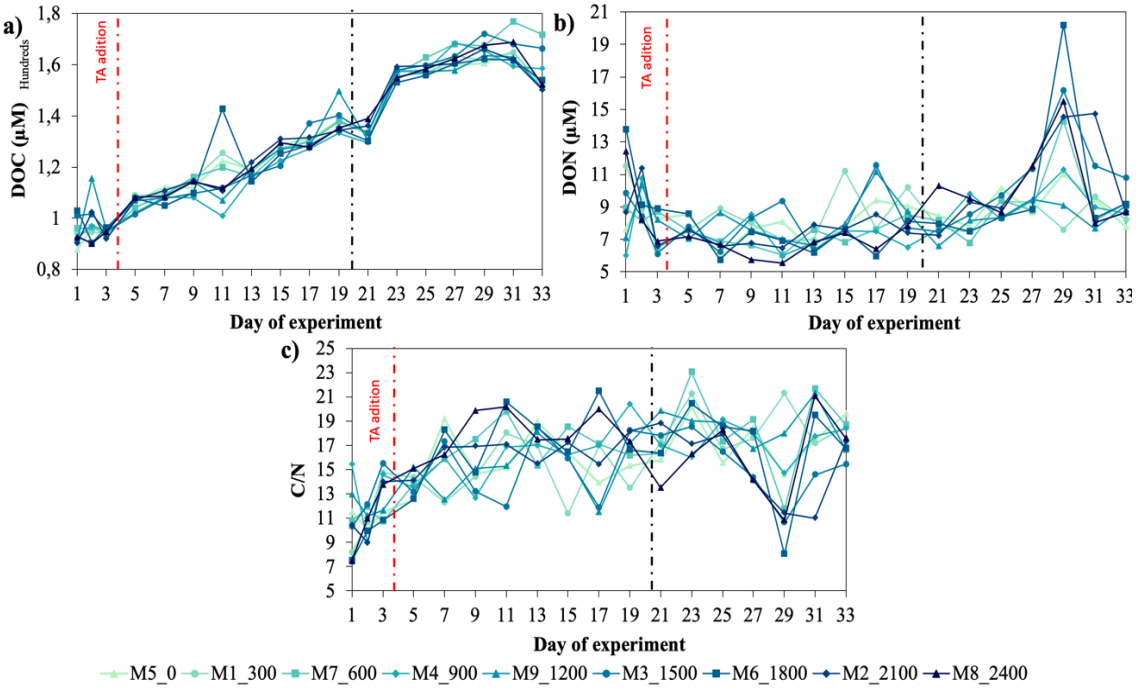

Figure 5. *Temporal development of (a and b) dissolved organic carbon (DOC) and nitrogen (DON), respectively, and (c) the ratio between both (C/N) over the course of the experiment for each mesocosm (M). The x-axis represents the number of days that have passed since the commencement of the experiment. Vertical dashed red line indicates the day of TA manipulation and beginning of phase 1. Vertical dashed black line delimits phase 1 from phase 2.*

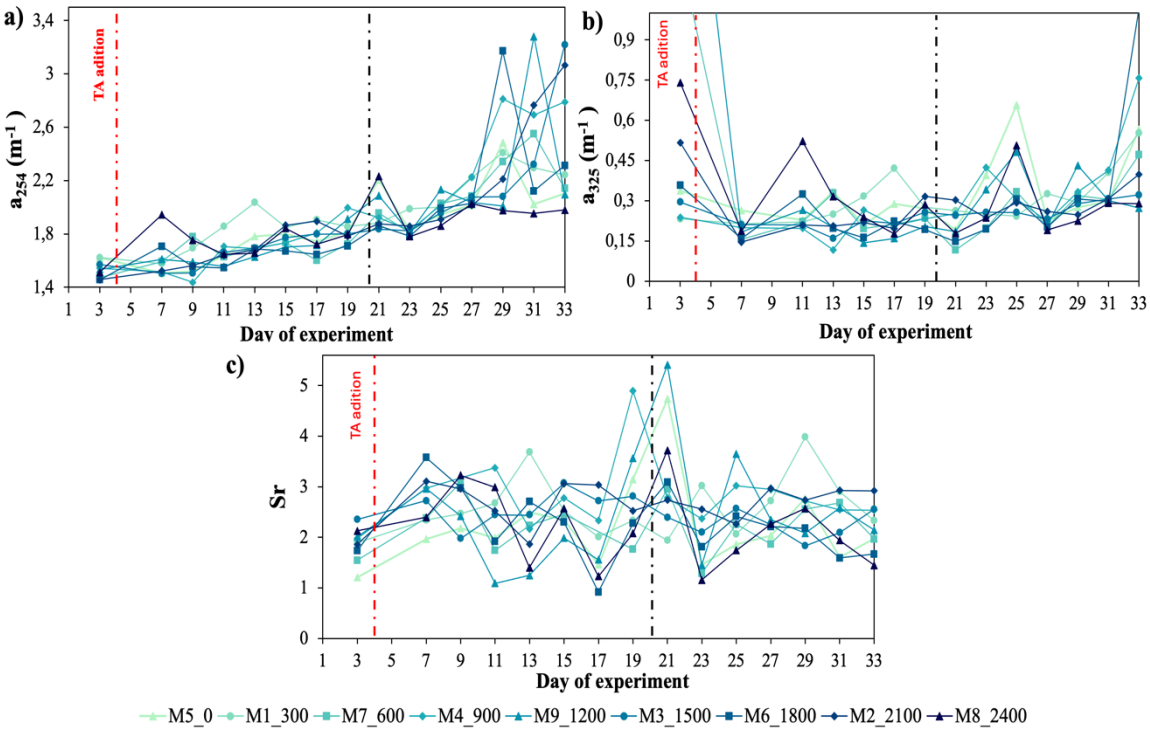

Figure 6. *Temporal development of the coefficient of absorbance at wavelength of (a)254 nm (a_{254}) and (b) 325 nm (a_{325}), and (c) the ratio of the slopes between 275-295 nm and 350-400 nm (Sr) over the course of the experiment for each mesocosm. The x-axis represents the number of days that have passed since the commencement of the experiment. Vertical dashed red line indicates the day of TA manipulation and beginning of phase 1. Vertical dashed black line delimits phase 1 from phase 2.*

3.4. Temporal development of prokaryotic community

Figures 7a and 7b illustrate the concentrations of high nucleic acid (HNA) and low nucleic acid (LNA) content bacteria, respectively. During the initial phase, the concentrations of HNA remained relatively constant, with no notable differences observed among the mesocosms. In contrast, the concentrations of LNA decreased following the addition of TA until the onset of the second phase. Although differences were observed among the mesocosms, they were not related to TA (Table 2). In Phase II, both HNA and LNA exhibited a similar trend, demonstrating a rapid increase in M3, M4, M6, and M7 during the Chla bloom. While M2, M5, M1, M6, and M9 declined after day 29, reaching values comparable to those observed in Phase I, M1 and M7 continued to grow until the conclusion of the experiment.

The total HB concentrations demonstrate a comparable declining trend to that of LNA in phase I (Fig. 7b and Fig. 7c). This, in conjunction with the stable concentrations of HNA, resulted in an increase in the HNA/LNA ratio during this period (Fig. 7a and fig. 7d). Similarly to HNA and LNA, the concentration of HB increased in the second phase, reaching its maximum value on day 29. Conversely, the HNA/LNA ratio remained stable in all mesocosms, except in the two lowest TA treatments, in which the ratio increased until the end of the experiment. No significant TA effect was observed on HB, HNA, LNA, or the ratio between the former two (Table 2).

Table 2. *Reduced Major Axis regressions (model II) statistics of the relationship between log-transformed DIC concentrations with* LNA, HNA, HB, DOC, DON, a_{325}, a_{254}, S_r, and Chla. *Significant correlations are indicated with ** (p-value<0.05) * 0.05<p-value>0.10.*

	Phase I			Phase II		
	Slope	r^2	p-value	Slope	r^2	p-value
LNA	-	0.01	0.43	+	0.01	0.48

HNA	-	0.13	0.16	+	0.06	0.60
HB	-	0.05	0.29	+	0.08	0.54
DOC	-	0.03	0.32	-	0.01	0.94
DON	-	**0.29**	**0.06***	+	**0.31**	**0.09***
a_{325}	-	0.09	0.21	+	**0.30**	**0.10***
a_{254}	-	0.02	0.35	+	0.26	0.25
S_r	+	0.04	0.30	-	0.05	0.61
Chla	-	0.13	0.42	+	**0.61**	**0.02***

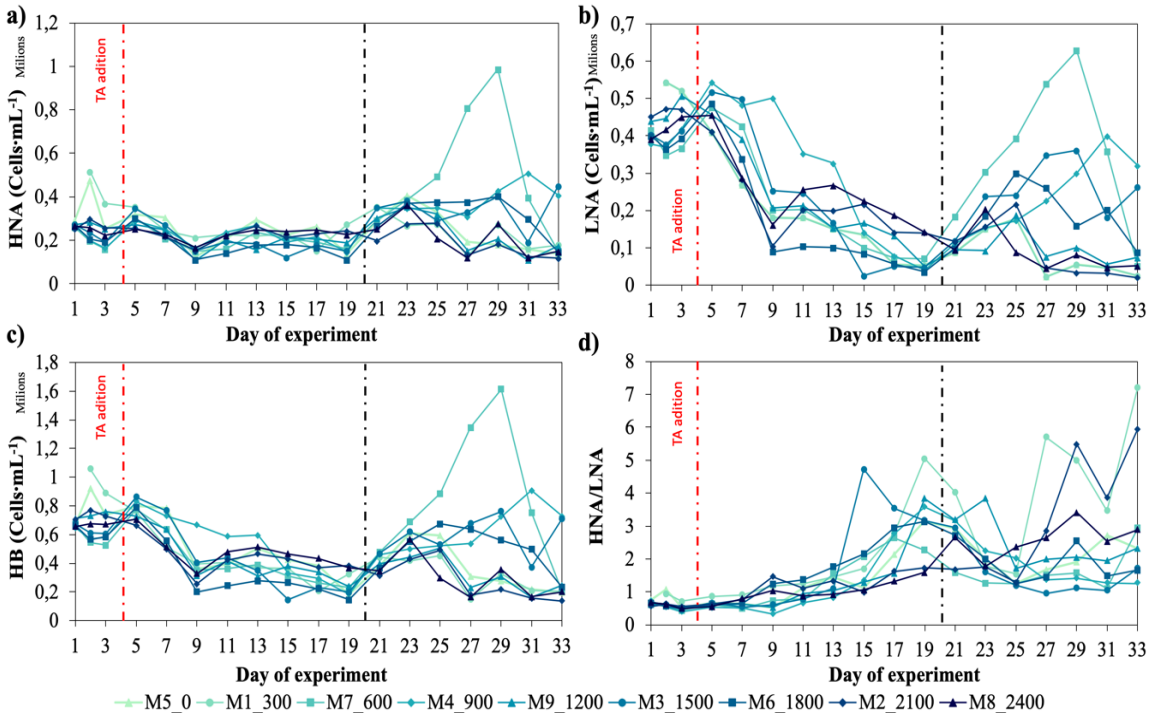

***Figure 7**. Temporal development of (a)high and (b) low nucleic acid content bacteria abundances (HNA and LNA, respectively), (c) total heterotrophic bacteria abundance (HB), and (d) the ratio between HNA and LNA bacteria, over the course of the experiment for each mesocosm (M). The x-axis represents the number of days that have passed since the beginning of the experiment. Vertical dashed red line indicates the day of TA manipulation and beginning of phase 1. Vertical dashed black line delimits phase 1 from phase 2.*

4. DISCUSION

The alterations in the inorganic carbon chemistry associated with Ocean Alkalinity Enhancement (OAE) may have significant implications for oceanic planktonic communities. It is therefore imperative to gain an understanding of the way in which this approach affects marine ecosystems, with a view to assessing their viability and

minimizing potential unintended effects, prior to its implementation on a larger scale. Given the pivotal role of marine heterotrophic bacteria in nutrient and organic matter cycling (Azam, 1998), it is crucial to know whether changes in oceanic TA will also influence the dynamics of the bacterioplankton in the sea. In this regard, the OAE simulation conducted in the present study, based on CO_2–equilibrated alkalinity gradients, permitted the establishment and maintenance of different TA levels in a natural oligotrophic plankton assemblage, thereby providing detailed insights into the potential outcomes under controlled experimental conditions.

4.1. Temporal dynamics: Discrepancy between DOC and Primary Production

Initial concentration of both organic matter and prokaryotic abundances were similar to those typically found in surface waters of the Canary Island oceanic regions (Arístegui et al., 2003, 2020; Baltar et al., 2007). Concentrations of DOC quickly increased in all mesocosm after TA addition reaching ~150 µM by the end of phase II on day 20. The main source of DOC in the ocean is exudation by primary producers (Lønborg et al., 2009, 2020; Nagata, 2000). Enhanced photosynthesis alongside the absence of physical processes within the mesocosms may result in the accumulation of large amounts of DOC as previously observed by Gómez-Letona et al. (2022) in other mesocosms study conducted in the same location. However, the concentration of Chla remained relatively stable throughout the entirety of Phase I of this study, indicating that there was no substantial growth of the phytoplankton community. The findings of Marín-Samper et al. (2024), which represent a more comprehensive investigation of primary production within the same experiment, are in alignment with our observations. They documented low and stable gross (GP) and net community production (NCP) during phase I, and additionally reported GP to community respiration r (CR) ratios of approximately 1 for the same period, indicating a near equilibrium between production and respiration.

This discrepancy between DOC and primary production gives rise to the question of the source of the accumulated organic carbon. Other DOC sources such as extracellular release, zooplankton sloppy feeding, and viral cell lysis of host organisms may contribute to DOC production in the ocean (Nagata, 2000). The results reported by Marín-Samper et al. (2024) suggest that extracellular release is an insufficient explanation for the observed DOC levels in our study. They observed low ^{14}C-labelled DOC production during the phase I. Indeed, accumulated DO^{14}C production by the end of the phase I was

0.69±0.10 µM while by the same point of the experiment DOC had increased by 38.75±6.39 µM. The zooplankton does not seem to be able to explain it on its own either. Meso- and microzooplankton remained very low during the whole experiment, decreasing from day 1 to the end of the phase I (unpublished data).

Viral lysis, on the other hand, may help to explain the observed DOC accumulation. Viral cell lysis promptly affects the standing stock of DOC by destroying host cells and releasing their content as dissolved bioavailable components (Brussaard et al., 2008; Lønborg et al., 2013). Thus, viral infection and the concomitant cell lysis redirect biomass away from grazers towards bacteria (which may explain the low zooplankton abundances), a process known as the "viral shunt" (Wilhelm and Suttle, 1999). Most marine viruses are thought to be bacteriophages, which would explain the decay of the HB during the first phase. Most likely, the combination of viral activity, $DO^{14}C$ production and zooplankton feeding, together with reduced DOC consumption and lack of ventilation inside the mesocosms, could then lead to the observed DOC accumulation during Phase I.

During phase II, the rate of DOC accumulation accelerated, coinciding with the peak in Chla, but decreased thereafter alongside the increase in PP. The growth of HB during phase II, together with increased respiration, may have resulted in DOC consumption, slowing its accumulation. In fact, the GP:CR ratio reported by Marín-Samper et al. (2024) was less than 1 in several mesocosms during this phase.

4.2. Temporal dynamics: Growth under nutrient limitation

One of the most notable outcomes of this study is the development of a nutrient-decoupled phytoplankton bloom in selected mesocosms during Phase II. Despite comparable measured inorganic nutrient levels to those observed in Phase I, Chla was, in some cases, up to one order of magnitude higher. A bloom of such magnitude has not been observed in previous mesocosms experiments conducted in the same location under nutrient-deplete conditions, nor in experimental phases simulating ocean acidification where modifications were made to seawater carbonate chemistry (pH, pCO_2)(Hernández-Hernández et al., 2018; Bacht et al., 2019). Furthermore, HB also showed an increase in abundance during Phase II, despite the presence of comparable organic and inorganic nutrients in both phases.

The observed correlation between the intensity of the bloom and the concentration of TA precludes the possibility that this phenomenon is a random or coincidental occurrence. It should be noted that there was no TA effect on HB increase. Paul et al. (2024) proposed two potential explanations for this anomalous phenomenon with respect to primary production. On the one hand, they suggest that extracellular pH may influences phytoplankton nutrient uptake, and thereby enable such blooms under the observed nutrient-poor conditions. However, there are poor constraints on how pH levels in the extracellular microenvironment surrounding phytoplankton cells (the phycosphere) differ from bulk seawater. In addition, although it is known to affect iron consumption, little is known about its role in inorganic nutrient uptake (Liu et al., 2022; Coale et al., 2019). On the other hand, they put forth a hypothesis wherein the heterotrophic bacterial community is influenced by OAE, particularly with regard to its organic nitrogen turnover capacity. The data presented here are inconsistent with the aforementioned hypothesis. No effect of TA was observed in the abundance of HB community. While it is true that similar to the findings of Paul et al. (2024) in the particulate fraction, a relationship between DON, and C/N dynamics and TA concentration were identified, supporting the idea of a TA effects on heterotrophic nitrogen turnover. It should be noted that this hypothesis was formulated before the data collected in this work were available, and therefore they were unaware of the information we provided.

Based on our results, we proposed a third hypothesis to explain the nutrient-decoupled bloom. As explained in the previous section, viral lysis may have played an important role during phase I. It is well documented that virus-mediated destruction of microorgansism facilitates carbon and nutrient exchange between trophic classes of microorganisms—autotrophs and heterotrophs (Willhelm and Suttle, 1999; Locke et al., 2022; Shelford and Suttle, 2018). Shelford and Suttle (2018), in laboratory experiment, observed that DON released as the results of viral lysis was metabolized by uninfected bacteria, producing ammonium that supported phytoplankton growth. This explanation would fit our scenario. Viral lysis during phase I would enhance the recycling of DON by HB into NH_4 (not measured in this experiment) which accumulated supporting the later development of phytoplankton bloom in phase II. The fact that particulate nitrogen was poorly enriched with ^{15}N in blooming mesocosms, which indicates the use of a different nitrogen source than NO_3 (Paul et al., 2024), support our hypothesis. Furthermore, it would be in agreement with the effects on N turnover observer in our

study and by Paul et al. (2024). The reason for the observed correlation between the intensity of bloom and the concentration of TA, despite the absence of any effect of TA on HB, can be attributed to the influence of DIC. The actual CO_2-limitation of the Ribulose-1,5-biphosphate carboxylase/oxygenase (RubisCO) enzyme (Beardal and Raven, 2004; Reinfelder, 2011; Mackey et al., 2015) would be alleviated as TA levels increase. However, what ultimately triggers the bloom and the temporal coincidence with $CaCO_3$ precipitation remains unclear.

4.3. TA-related effects

Of the parameters examined in this experiment, only DON demonstrated a weak TA-related effect during the initial phase. As mentioned in the section before, this agrees with Paul et al. (2024) results, which observed the same impact in PON. As neither the phytoplankton community nor the heterotrophic community exhibits an effect of TA during the initial phase, the question of which process is responsible for the observed decline in organic N with increasing TA concentrations remains unanswered. Conversely, in the second phase, the DON demonstrates a positive impact of the TA, which this time may be associated with the same effect observed by Marín-Samper et al (2024) in the PP. Furthermore, the lack of effect on the heterotrophic community contradicts the results of Federer et al. (2022) who suggested that these communities are more sensitive to OAE than autotrophic communities.

CONCLUSION

The goal of this work was to test the impact of pre-equilibrated OAE on oligotrophic heterotrophic bacteria communities and their role in the marine biogeochemistry. Our findings indicates that under a nutrient limitation scenario pelagic heterotrophic bacteria are insensitive to increasing TA, as well as the pools of dissolved organic carbon. N-cycling, in the other hand, seem to be affected by OAE yet the mechanisms behind needs for further investigation. This provides increased confidence that even with a doubling of seawater alkalinity, the risk of significant changes in biogeochemical functioning remains low.

Furthermore, our results suggest that viral dynamics could play an important role in the unusual accumulation of DOC inside the mesocosms, and the nutrient-decoupled development of a phytoplankton bloom. Thus, it will be crucial to thoroughly investigate the underlying mechanisms, since this suggests that a potential side effect of alkalinity

enhancement could increase ecosystem productivity and alleviation of nutrient limitation in highly oligotrophic regions, which may affect the effectiveness of OAE implementation.

SUPPLEMENTARY

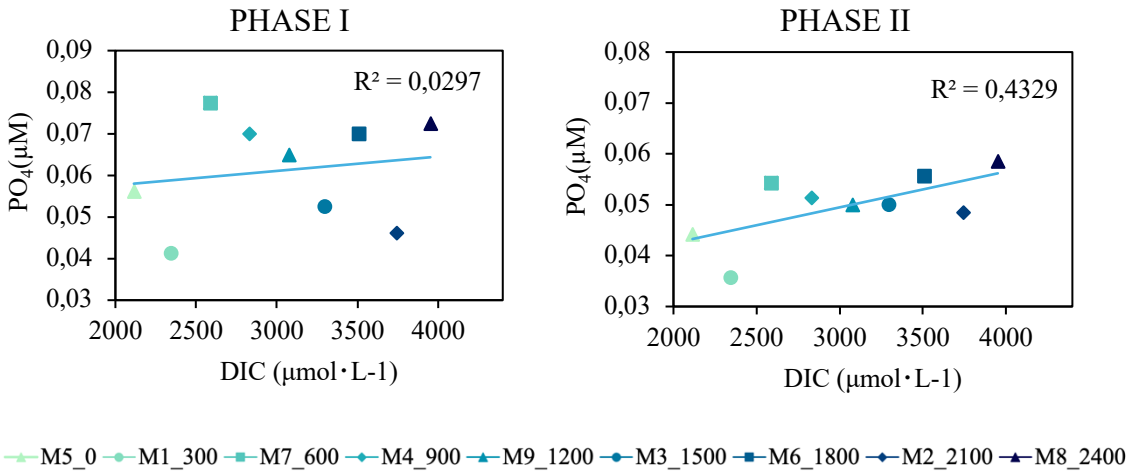

Figure S1. Linear regressions between ΔTA treatment and PO_4 per phase a) phase I, b) phase II. Mesocosms corresponds to mesocosm and ΔTA to 1 total alkalinity.

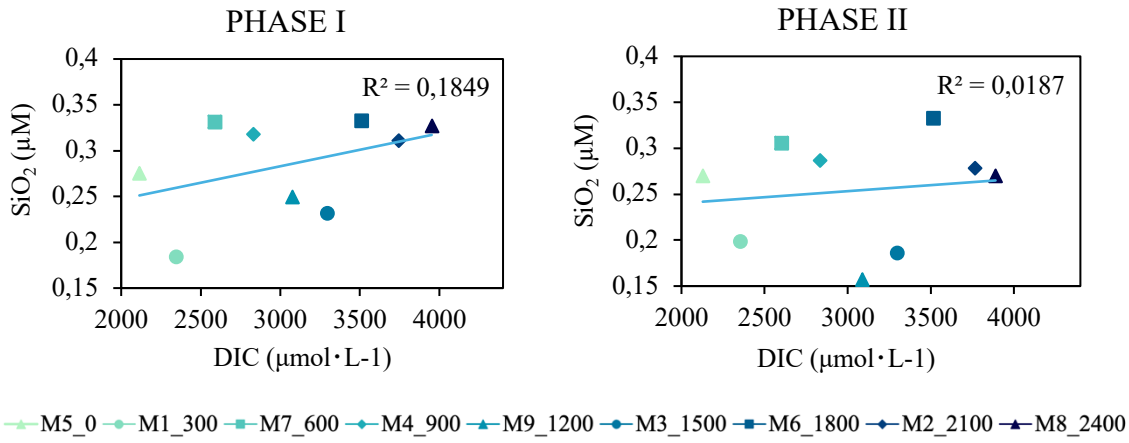

Figure S2. Linear regressions between ΔTA treatment and SiO_2 per phase a) phase I, b) phase II. Mesocosms corresponds to mesocosm and ΔTA to 1 total alkalinity.

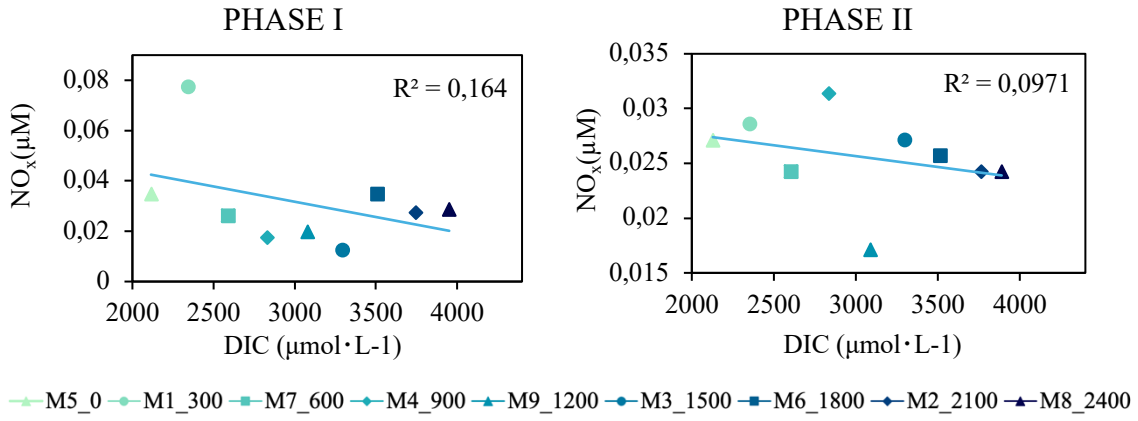

Figure S3. Linear regressions between ΔTA treatment and NO_x per phase a) phase I, b) phase II. Mesocosms corresponds to mesocosm and ΔTA to 1 total alkalinity.

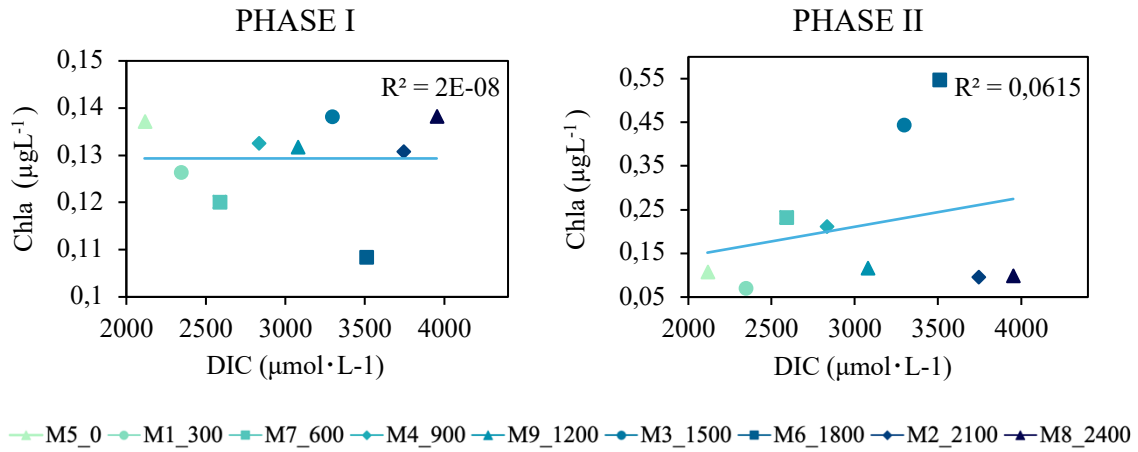

Figure S4. Linear regressions between ΔTA treatment and Chla per phase a) phase I, b) phase II. Mesocosms corresponds to mesocosm and ΔTA to 1 total alkalinity.

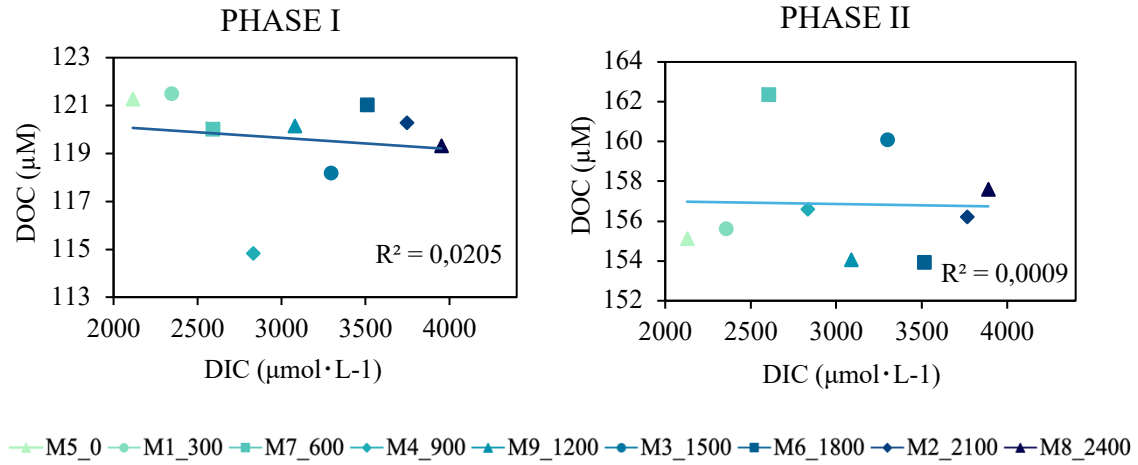

Figure S5. Linear regressions between ΔTA treatment and DOC per phase a) phase I, b) phase II. Mesocosms corresponds to mesocosm and ΔTA to 1 total alkalinity.

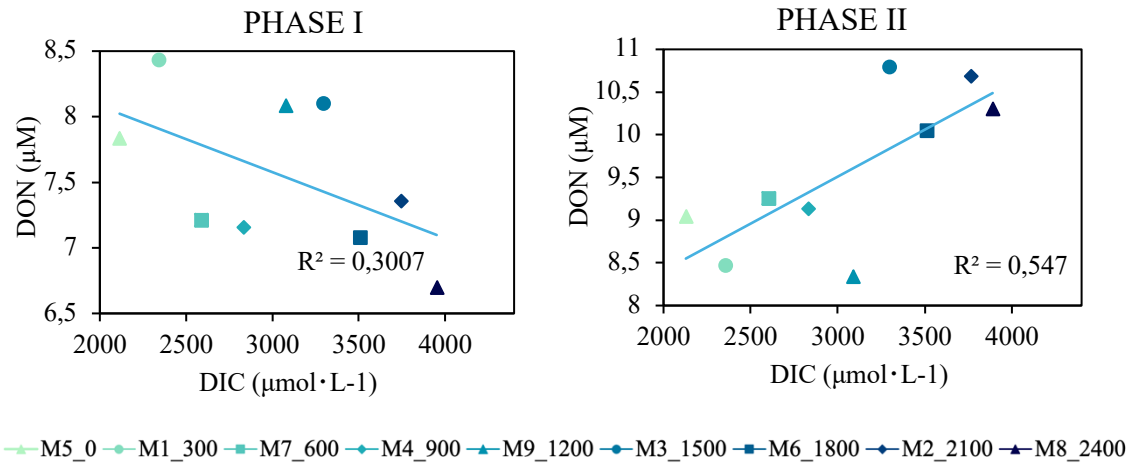

Figure S6. Linear regressions between ΔTA treatment and DON per phase a) phase I, b) phase II. Mesocosms corresponds to mesocosm and ΔTA to 1 total alkalinity.

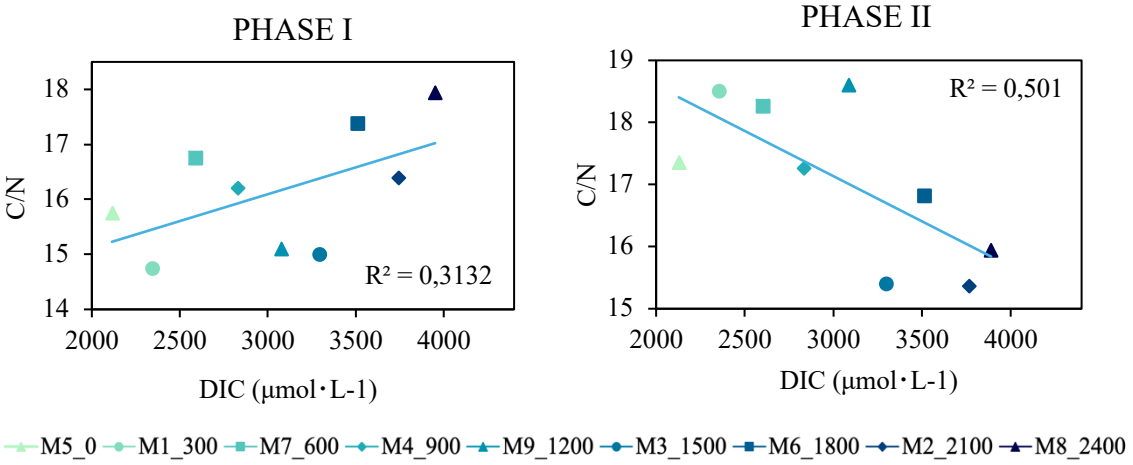

Figure S7. Linear regressions between ΔTA treatment and C/N per phase a) phase I, b) phase II. Mesocosms corresponds to mesocosm and ΔTA to 1 total alkalinity.

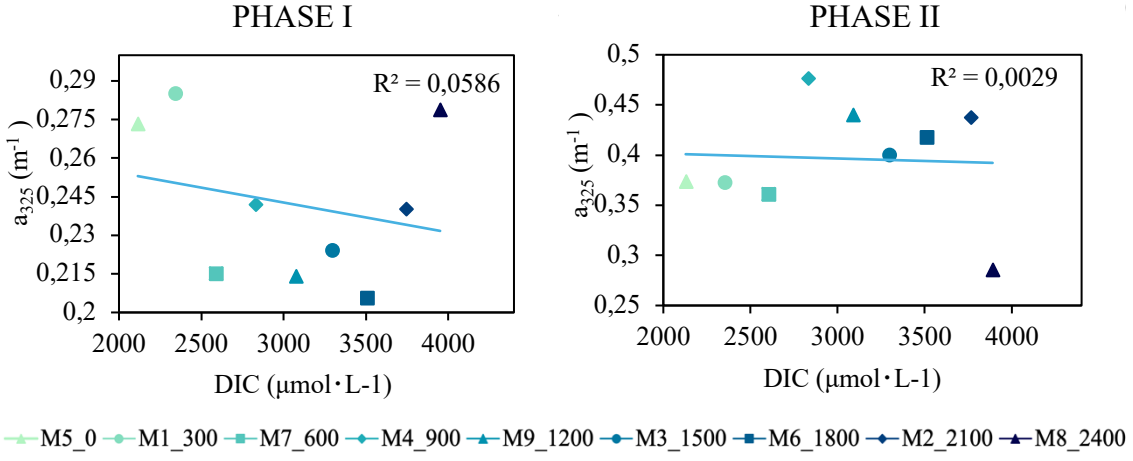

Figure S8. Linear regressions between ΔTA treatment and a_{325} per phase a) phase I, b) phase II. Mesocosms corresponds to mesocosm and ΔTA to 1 total alkalinity.

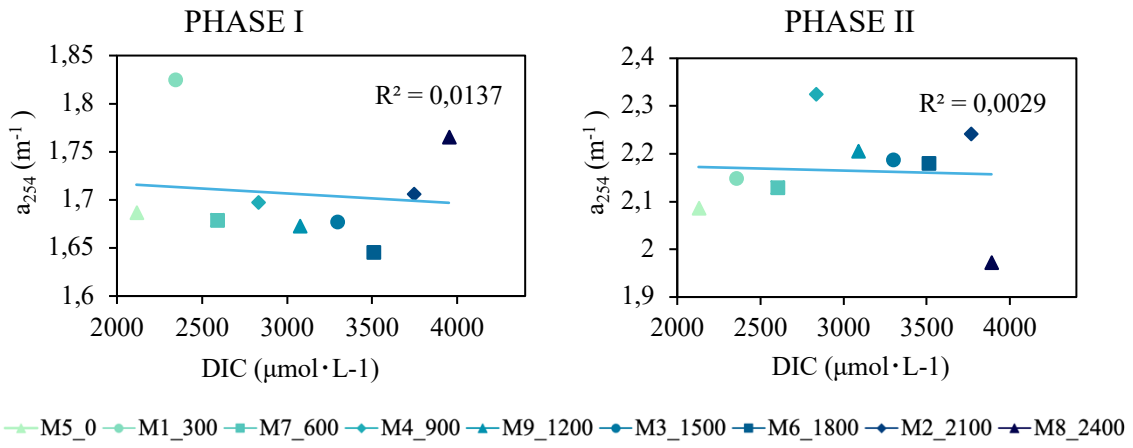

Figure S9. Linear regressions between ΔTA treatment and a_{254} per phase a) phase I, b) phase II. Mesocosms corresponds to mesocosm and ΔTA to 1 total alkalinity.

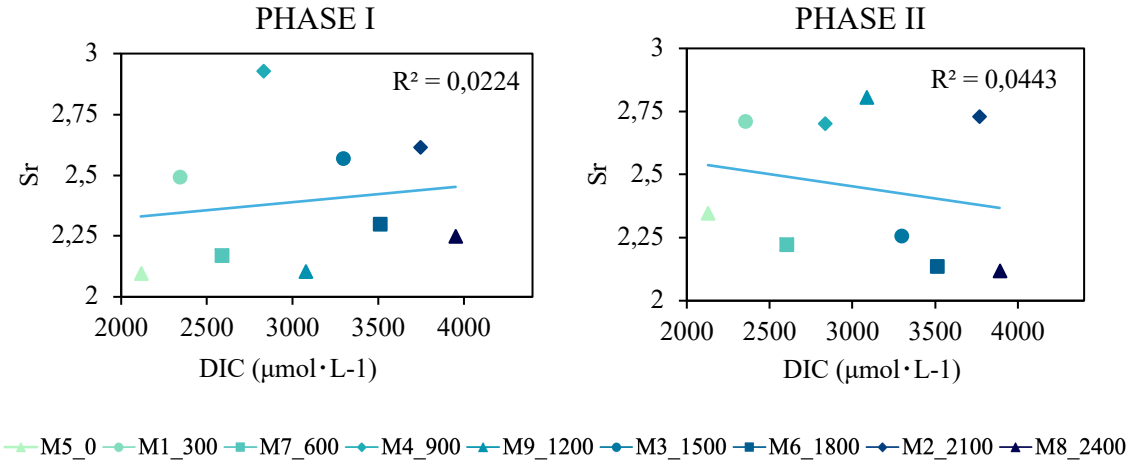

Figure S10. Linear regressions between ΔTA treatment and Sr per phase a) phase I, b) phase II. Mesocosms corresponds to mesocosm and ΔTA to 1 total alkalinity.

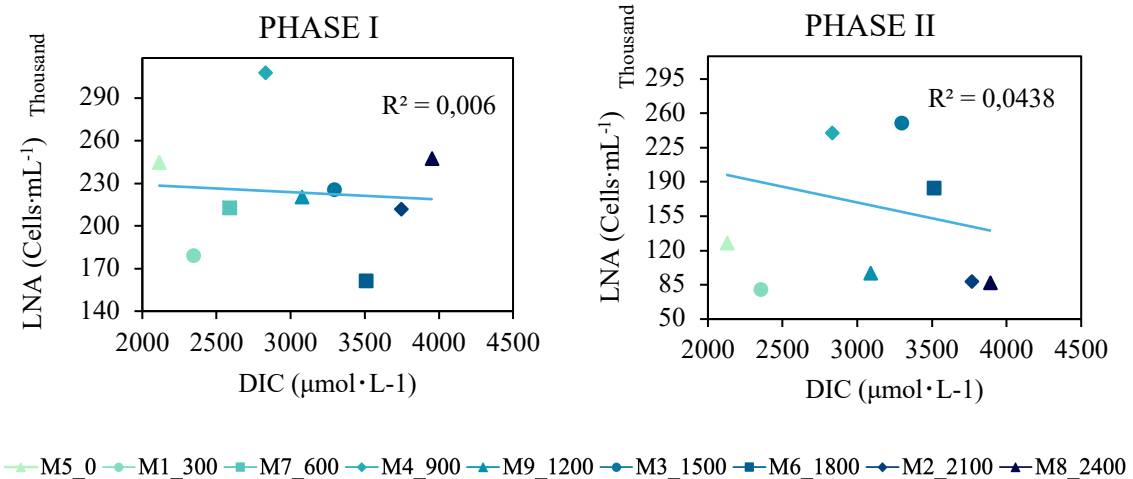

Figure S11. Linear regressions between ΔTA treatment and LNA per phase a) phase I, b) phase II. Mesocosms corresponds to mesocosm and ΔTA to 1 total alkalinity.

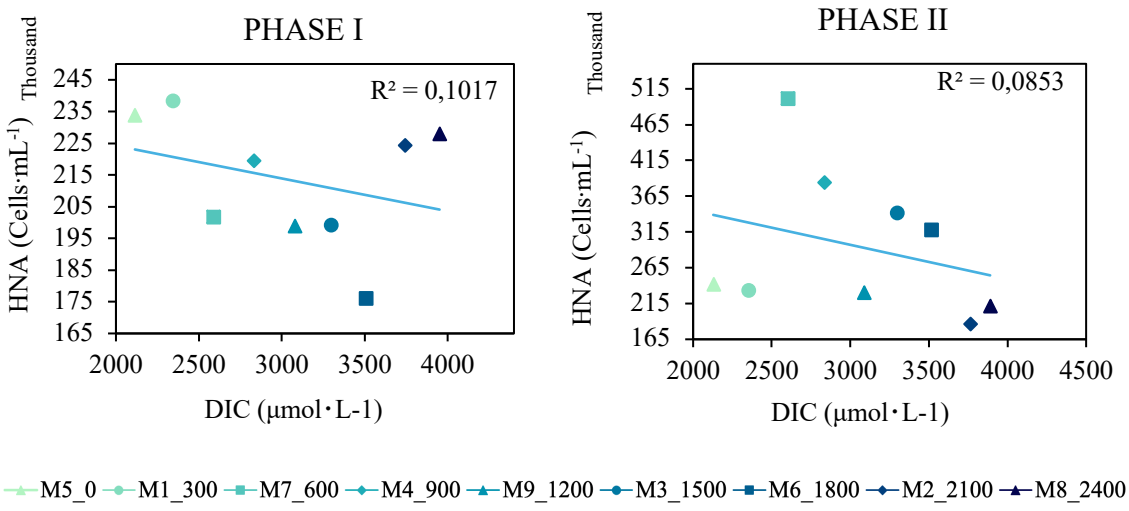

Figure S12. Linear regressions between ΔTA treatment and HNA per phase a) phase I, b) phase II. Mesocosms corresponds to mesocosm and ΔTA to 1 total alkalinity.

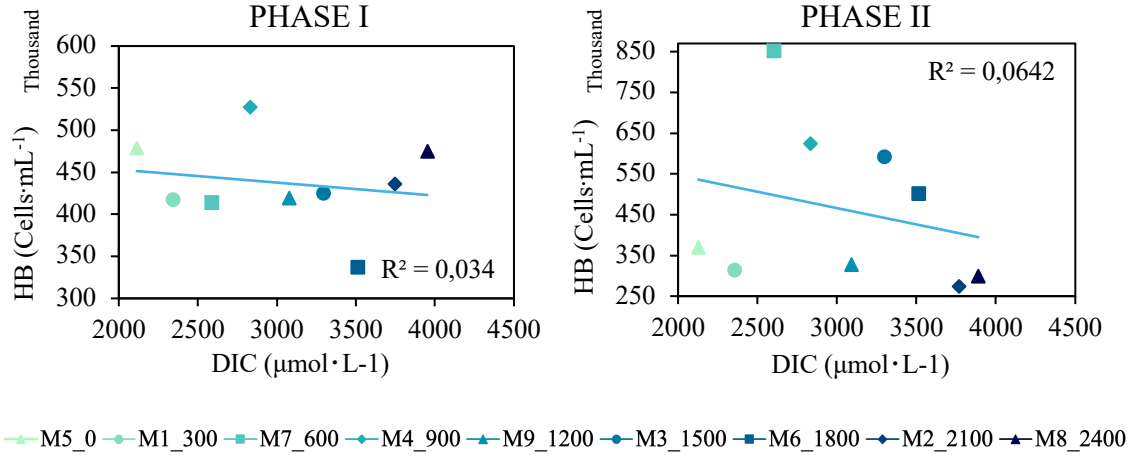

Figure S13. Linear regressions between ΔTA treatment and HB per phase a) phase I, b) phase II. Mesocosms corresponds to mesocosm and ΔTA to 1 total alkalinity.

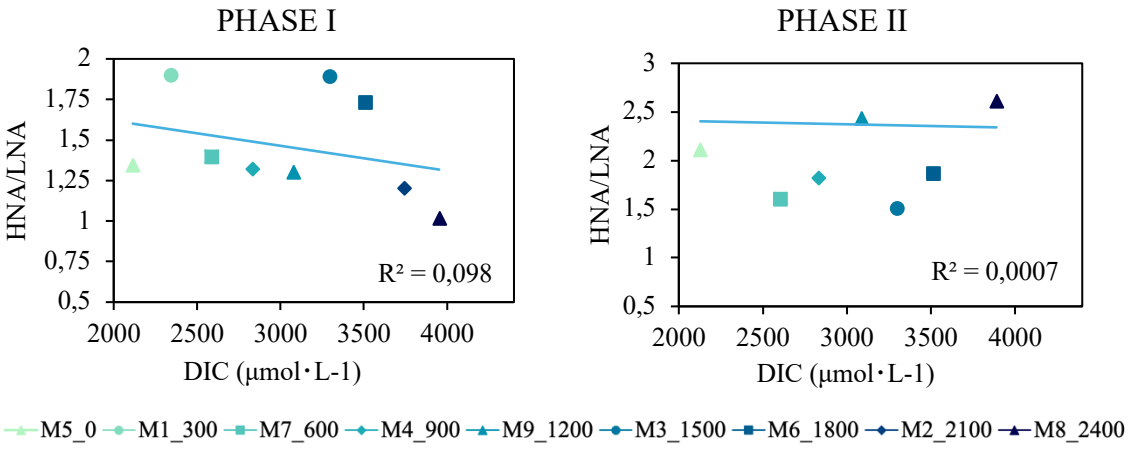

Figure S14. Linear regressions between ΔTA treatment and HNA/LNA per phase a) phase I, b) phase II. Mesocosms corresponds to mesocosm and ΔTA to 1 total alkalinity.

ACKNOWLEDGMENTS

I would like to express my sincerest gratitude to my two TFT supervisors, without whom I would not have received the indispensable support and knowledge necessary to develop this work, especially to Nauzet Hernandez, who was readily available for any minor inquiry, accompanying me throughout the process of growth and improvement. Furthermore, gratitude is extended to the Biological Oceanography Group of the ULPGC (GOB-ULPGC) for supplying the data that was instrumental in conducting this potentially significant work. I would like to express my sincerest gratitude to the KOSMOS team at GEOMAR for their invaluable technical and logistical support throughout the mesocosm experiment. Their coordination of in situ research activities and commitment to promoting fair data management and exchange were instrumental to the success of this work. Finally, we would like to acknowledge the Oceanic Platform of the Canary Islands (PLOCAN) and the University of Las Palmas de Gran Canaria (ULPGC) for providing the necessary facilities to conduct this experiment and, consequently, the development of this TFT. We extend our gratitude to all those who have provided invaluable support and contributions, which have been essential to this process.

BIBLIOGRAPHY

Arístegui, J., Barton, E. D., Montero, M. F., García-Muñoz, M., & Escánez, J. (2003). Organic carbon distribution and water column respiration in the NW Africa-Canaries coastal transition zone. *Aquatic Microbial Ecology, 33*, 289–301. https://doi.org/10.3354/ame033289

Arístegui, J., Montero, M. F., Hernández-Hernández, N., Alonso-González, I. J., Baltar, F., Calleja, M. L., et al. (2020). Variability in water-column respiration and its dependence on organic carbon sources in the Canary Current upwelling region. *Frontiers in Earth Science, 8*. https://doi.org/10.3389/feart.2020.00349

Bach, L. T., Alvarez-Fernandez, S., Hornick, T., Stuhr, A., & Riebesell, U. (2017). Simulated ocean acidification reveals winners and losers in coastal

phytoplankton. *PLOSONE, 12*(11), e0188198. https://doi.org/10.1371/journal.pone.0188198

Bach, L. T., Hernández-Hernández, N., Taucher, J., Spisla, C., Sforna, C., Riebesell, U., & Arístegui, J. (2019b). Effects of elevated CO_2 on a natural diatom community in the subtropical NE Atlantic. *Frontiers in Marine Science, 6*, Article 75. https://doi.org/10.3389/fmars.2019.00075

Baltar, F., Arístegui, J., Gasol, J. M., Hernández-León, S., & Herndl, G. J. (2007). Strong coast–ocean and surface–depth gradients in prokaryotic assemblage structure and activity in a coastal transition zone region. *Aquatic Microbial Ecology, 50*, 63–74

Beardall, J., & Raven, J. A. (2004). The potential effects of global climate change on microalgal photosynthesis, growth, and ecology. *Phycologia, 43*(1), 26–40. https://doi.org/10.2216/i0031-8884-43-1-26.1

Boesch, D. F., Field, J. C., & Scavia, D. (2000) *The potential consequences of climate variability and change on coastal areas and marine resources*. NOAA. http://www.cop.noaa.gov

Brussaard, C. P. D., Wilhelm, S. W., Thingstad, T. F., Weinbauer, M. G., Bratbak, G., Heldal, M., Kimmance, S. A., Middelboe, M., Nagasaki, K., Paul, J. H., Schroeder, D. C., Suttle, C. A., Vaque, D., & Wommack, K. E. (2008). Global scale processes with a nanoscale drive—the role of marine viruses. *ISME Journal, 2*(6), 575–578.

Burns, W., & Corbett, C. R. (2020). Antacids for the sea? Artificial ocean alkalinization and climate change. *One Earth, 3*(2), 154–156. https://doi.org/10.1016/j.oneear.2020.07.016

Coale, T. H., Moosburner, M., Horák, A., Oborník, M., Barbeau, K. A., & Allen, A. E. (2019). Reduction-dependent siderophore assimilation in a model pennate diatom. *Proceedings of the National Academy of Sciences of the United States of America, 116*(47), 23609–23617. https://doi.org/10.1073/pnas.1907234116

Dang, H. (2020). Grand challenges in microbe-driven marine carbon cycling research. *Frontiers in Microbiology, 11*, 1039. https://doi.org/10.3389/fmicb.2020.01039

Doney, S. C., Fabry, V. J., Feely, R. A., & Kleypas, J. A. (2009). Ocean acidification: The other CO_2 problem. *Annual Review of Marine Science, 1*, 169–192. https://doi.org/10.1146/annurev.marine.010908.163834

Azam, F. (1998). Microbial control of oceanic carbon flux: The plot thickens. *Science, 280*(5364), 694-696. https://doi.org/10.1126/science.280.5364.694

Feely, R. A., & Doney, S. C. (2011). Ocean Acidification: The Other CO2 Problem. *Limnology and Oceanography E-Lectures*. https://doi.org/10.4319/lol.2011.rfeely_sdoney.5

Ferderer, A., Chase, Z., Kennedy, F., Schulz, K. G., & Bach, L. T. (2022). Assessing the influence of ocean alkalinity enhancement on a coastal phytoplankton community. *Biogeosciences, 19*(10), 5375–5399. https://doi.org/10.5194/bg-19-5375-2022

Feng, E. Y., Koeve, W., Keller, D. P., & Oschlies, A. (2017). Model-based assessment of the CO_2 sequestration potential of coastal ocean alkalinization. *Earth's Future, 5*(12), 1252–1266. https://doi.org/10.1002/2017EF000659

Filella, A., Baños, I., Montero, M. F., Hernández-Hernández, N., Rodríguez-Santos, A., Ludwig, A., Riebesell, U., & Arístegui, J. (2018). Plankton community respiration and ETS activity under variable CO_2 and nutrient fertilization during a mesocosm study in the subtropical North Atlantic. *Frontiers in Marine Science, 5*, Article 310. https://doi.org/10.3389/fmars.2018.00310

Friedlingstein, P., Jones, M. W., O'Sullivan, M., Andrew, R. M., Bakker, D. C. E., Hauck, J., Le Quéré, C., Peters, G. P., Peters, W., Pongratz, J., Sitch, S., Canadell, J. G., Ciais, P., Jackson, R. B., Alin, S. R., Anthoni, P., Bates, N. R., Becker, M., Bellouin, N., … Zeng, J. (2022). Global carbon budget 2021. *Earth System Science Data, 14*(4), 1917–2005. https://doi.org/10.5194/essd-14-1917-2022

Fox, L., Stukins, S., Hill, T., & Miller, G. (2020). *CT data from Fox et al. 2020 quantifying the effect of anthropogenic climate change on calcifying plankton* [Data set]. Natural History Museum. https://doi.org/10.5519/0078402

Gafar, N. A., Eyre, B. D., & Schulz, K. G. (2018). A conceptual model for projecting coccolithophorid growth, calcification and photosynthetic carbon fixation rates in response to global ocean change. *Frontiers in Marine Science, 4*. https://doi.org/10.3389/fmars.2017.00433

Gao, Y., Zhang, Y., Du, M., Lin, F., & others. (2021). Dissolved organic carbon from cultured kelp *Saccharina japonica*: Production, bioavailability, and bacterial degradation rates. *Aquaculture Environment Interactions, 13*, 101–110. https://doi.org/10.3354/aei00393

Gattuso, J. P., Magnan, A. K., Bopp, L., Cheung, W. W. L., Duarte, C. M., Hinkel, J., McLeod, E., Micheli, F., Oschlies, A., Williamson, P., Billé, R., Chalastani, V. I., Gates, R. D., Irisson, J. O., Middelburg, J. J., Pörtner, H. O., & Rau, G. H. (2018). Ocean solutions to address climate change and its effects on marine ecosystems. *Frontiers in Marine Science, 5*, Article 337. https://doi.org/10.3389/fmars.2018.00337

Gattuso, J. P., Williamson, P., Duarte, C. M., & Magnan, A. K. (2021). The potential for ocean-based climate action: Negative emissions technologies and beyond. *Frontiers in Climate, 2*. https://doi.org/10.3389/fclim.2020.575716

Hall-Spencer, J. M., & Harvey, B. P. (2019). Ocean acidification impacts on coastal ecosystem services due to habitat degradation. *Emerging Topics in Life Sciences, 3*(2), 197–206. https://doi.org/10.1042/ETLS20180117

Hansen, H. P., & Koroleff, F. (1999). Determination of nutrients. En K. Grasshoff, K. Kremling, & M. Ehrhardt (Eds.), *Methods of seawater analysis* (3ª ed., pp. 159–226). Wiley-VCH. https://doi.org/10.1002/9783527613984.ch10

Hartmann, J., Suitner, N., Lim, C., Schneider, J., Marín-Samper, L., Arístegui, J., Renforth, P., Taucher, J., & Riebesell, U. (2023). Stability of alkalinity in ocean alkalinity enhancement (OAE) approaches - consequences for durability of CO_2 storage. *Biogeosciences, 20*(4), 781–802. https://doi.org/10.5194/bg-20-781-2023

Harvey, L. D. D. (2008). Mitigating the atmospheric CO_2 increase and ocean acidification by adding limestone powder to upwelling regions. *Journal of Geophysical Research: Oceans, 113*(4). https://doi.org/10.1029/2007JC004373

Haszeldine, R. S., Flude, S., Johnson, G., & Scott, V. (2018). Negative emissions technologies and carbon capture and storage to achieve the Paris Agreement commitments. *Philosophical Transactions of the Royal Society A: Mathematical, Physical and Engineering Sciences, 376*(2119). https://doi.org/10.1098/rsta.2016.0447

Helms, J. R., Stubbins, A., Ritchie, J. D., Minor, E. C., Kieber, D. J., & Mopper, K. (2008). Absorption spectral slopes and slope ratios as indicators of molecular weight, source, and photobleaching of chromophoric dissolved organic matter. *Limnology and Oceanography, 53*(3), 955–969. https://doi.org/10.4319/lo.2008.53.3.0955

Helms, J. R., Stubbins, A., Perdue, E. M., Green, N. W., Chen, H., & Mopper, K. (2013). Photochemical bleaching of oceanic dissolved organic matter and its effect on absorption spectral slope and fluorescence. *Marine Chemistry, 155*, 81–91. https://doi.org/10.1016/j.marchem.2013.05.015

Hernández-Hernández, N., Bach, L. T., Montero, M. F., Taucher, J., Baños, I., Guan, W., Espósito, M., Ludwig, A., Achterberg, E. P., Riebesell, U., & Arístegui, J. (2018). High CO_2 under nutrient fertilization increases primary production and biomass in subtropical phytoplankton communities: *A mesocosm approach. Frontiers in Marine Science, 5, 213. https://doi.org/10.3389/fmars.2018.00213*

Hornick, T., Bach, L. T., Crawfurd, K. J., Spilling, K., Achterberg, E. P., Woodhouse, J. N., Schulz, K. G., Brussaard, C. P. D., Riebesell, U., & Grossart, H. P. (2017a). *Ocean acidification impacts bacteria-phytoplankton coupling at low-nutrient conditions. Biogeosciences, 14(1), 1–15. https://doi.org/10.5194/bg-14-1-2017*

Hornick, T., Bach, L. T., Crawfurd, K. J., Spilling, K., Achterberg, E. P., Woodhouse, J. N., Schulz, K. G., Brussaard, C. P. D., Riebesell, U., & Grossart, H. P. (2017b). Ocean acidification impacts bacteria-phytoplankton coupling at low-nutrient conditions. *Biogeosciences, 14*(1), 1–15. https://doi.org/10.5194/bg-14-1-2017

Huo, C. L., Huo, C., & Guan, D. M. (2013). Advances in studies of ocean acidification. *Applied Mechanics and Materials, 295–298*, 2191–2194. https://doi.org/10.4028/www.scientific.net/amm.295-298.2191

IPCC. (2014). *Climate Change 2014: Synthesis Report. Contribution of Working Groups I, II and III to the Fifth Assessment Report of the Intergovernmental Panel on Climate Change.* IPCC. https://www.ipcc.ch/report/ar5/syr/

IPCC. (2018). *Global Warming of 1.5°C. An IPCC Special Report on the impacts of global warming of 1.5°C above pre-industrial levels and related global greenhouse gas emission pathways, in the context of strengthening the global response to the threat of climate change, sustainable development, and efforts to eradicate poverty.* IPCC. https://www.ipcc.ch/sr15/

IPCC. (2019). *Climate Change and Land: An IPCC special report on climate change, desertification, land degradation, sustainable land management, food security, and greenhouse gas fluxes in terrestrial ecosystems.* IPCC. https://www.ipcc.ch/srccl/

IPCC. (2020). *IPCC Special Report on the Ocean and Cryosphere in a Changing Climate.* IPCC. https://www.ipcc.ch/srocc/

Ji, X., Jiang, M., Zhang, J., Jiang, X., & Zheng, Z. (2018). The interactions of algae-bacteria symbiotic system and its effects on nutrients removal from synthetic wastewater. *Bioresource Technology*, *247*, 44–50. https://doi.org/10.1016/j.biortech.2017.09.074

Kheshgi, H. S. (1995). Sequestering atmospheric carbon dioxide by increasing ocean alkalinity. *Energy, 20*(9), 915–922.

Liu, F., Gledhill, M., Tan, Q. G., & Others. (2022). Phycosphere pH of unicellular nano- and micro-phytoplankton cells and consequences for iron speciation. *ISME Journal, 16*, 2329–2336. https://doi.org/10.1038/s41396-022-01280-1

Locke, H., Bidle, K. D., Thamatrakoln, K., Johns, C. T., Bonachela, J. A., Ferrell, B. D., & Wommack, K. E. (2022). Marine viruses and climate change: Virioplankton, the carbon cycle, and our future ocean. In M. J. Roossinck (Ed.), *Advances in Virus Research* (Vol. 114, pp. 67–146). Academic Press. https://doi.org/10.1016/bs.aivir.2022.09.001

Lønborg, C., Álvarez-Salgado, X. A., Davidson, K., & Miller, A. E. J. (2009). Production of bioavailable and refractory dissolved organic matter by coastal heterotrophic microbial populations. *Estuarine, Coastal and Shelf Science, 82*, 682–688. https://doi.org/10.1016/j.ecss.2009.02.026

Lønborg, C., Middelboe, M., & Brussaard, C. P. D. (2013). Viral lysis of *Micromonas pusilla*: Impacts on dissolved organic matter production and composition. *Biogeochemistry, 116*(1), 231–240. https://doi.org/10.1007/s10533-013-9853-1

Lønborg, C., Carreira, C., Jickells, T., & Álvarez-Salgado, X. A. (2020). Impacts of global change on ocean dissolved organic carbon (DOC) cycling. *Frontiers in Marine Science, 7*, 466. https://doi.org/10.3389/fmars.2020.00466

Lueker, T. J., Dickson, A. G., & Keeling, C. D. (2000). Ocean pCO calculated from dissolved inorganic carbon, 2 alkalinity, and equations for K and K : validation based on 1 2 laboratory measurements of CO in gas and seawater at 2 equilibrium. In *Marine Chemistry* (Vol. 70). www.elsevier.nlrlocatermarchem.

Mackey, K. R. M., Morris, J. J., Morel, F. M. M., & Kranz, S. A. (2015). Response of photosynthesis to ocean acidification. *Oceanography, 28*(2), 74–91. https://doi.org/10.5670/oceanog.2015.33

Marín-Samper, L., Arístegui, J., Hernández-Hernández, N., Ortiz, J., Archer, S. D., Ludwig, A., & Riebesell, U. (2024a). Assessing the impact of CO2-equilibrated ocean alkalinity enhancement on microbial metabolic rates in an oligotrophic system. *Biogeosciences*, *21*(11), 2859–2876. https://doi.org/10.5194/bg-21-2859-2024.

Marín-Samper, L., Arístegui, J., Hernández-Hernández, N., Ortiz, J., Archer, S. D., Ludwig, A., & Riebesell, U. (2024b). Assessing the impact of CO2-equilibrated ocean alkalinity enhancement on microbial metabolic rates in an oligotrophic system. *Biogeosciences*, *21*(11), 2859–2876. https://doi.org/10.5194/bg-21-2859-2024.

Nagata, T. (2000). Production mechanisms of dissolved organic carbon. In D. L. Kirchman (Ed.), *Microbial ecology of the oceans* (Vol. 1, pp. 121–153). Wiley-Liss.

Nzila, A., & Musa, M. M. (2021). Current status of and future perspectives in bacterial degradation of benzo[a]pyrene. *International Journal of Environmental Research and Public Health*, *18*(1), 1–24. https://doi.org/10.3390/ijerph18010262

Ruvalcaba Baroni, I., Palastanga, V., & Slomp, C. P. (2020). Enhanced organic carbon burial in sediments of oxygen minimum zones upon ocean deoxygenation. *Frontiers in Marine Science, 6*, Article 839. https://doi.org/10.3389/fmars.2019.00839

Orr, J. C., Fabry, V. J., Aumont, O., Bopp, L., Doney, S. C., Feely, R. A., ... Yool, A. (2005). Anthropogenic ocean acidification over the twenty-first century and its impact on calcifying organisms. *Nature, 437*(7059), 681–686. https://doi.org/10.1038/nature04095

Paul, A. J., Haunost, M., Goldenberg, S. U., Hartmann, J., Sánchez, N., Schneider, J., Suitner, N., & Riebesell, U. (2024). Ocean alkalinity enhancement in an open ocean ecosystem: Biogeochemical responses and carbon storage durability. *EGUsphere* [preprint]. https://doi.org/10.5194/egusphere-2024-417

Piontek, J., Lunau, M., Händel, N., Borchard, C., Wurst, M., & Engel, A. (2010). Acidification increases microbial polysaccharide degradation in the ocean. *Biogeosciences*, *7*(5), 1615–1624. https://doi.org/10.5194/bg-7-1615-2010

R Core Team. (2021). *R: A language and environment for statistical computing*. R Foundation for Statistical Computing. https://www.R-project.org/

Rama, R., Ode Muhammad Aslan, L., Iba, W., Nurdin, A. R., Armin, A., & Yusnaeni, Y. (2018). Seaweed cultivation of micropropagated seaweed (*Kappaphycus alvarezii*) in Bungin Permai coastal waters, Tinanggea sub-district, South Konawe Regency, South East Sulawesi. *IOP Conference Series: Earth and Environmental Science, 175*(1), Article 012219. https://doi.org/10.1088/1755-1315/175/1/012219

Reinfelder, J. R. (2011). Carbon concentrating mechanisms in eukaryotic marine phytoplankton. *Annual Review of Marine Science, 3*(1), 291–315. https://doi.org/10.1146/annurev-marine-120709-142720

Renforth, P., Jenkins, B. G., & Kruger, T. (2013). Engineering challenges of ocean liming. *Energy*, *60*, 442–452. https://doi.org/10.1016/j.energy.2013.08.006

Riebesell, U., Schulz, K., Bellerby, R., … & E. Zöllner. (2007). Enhanced biological carbon consumption in a high CO2 ocean. *Nature, 450*(7169), 545–548. https://doi.org/10.1038/nature06267

Rockström, J., Steffen, W., Noone, K., Persson, Å., Chapin, F. S., Lambin, E., Lenton, T. M., Scheffer, M., Folke, C., Schellnhuber, H., Nykvist, B., De Wit, C. A., Hughes, T., Van Der Leeuw, S., Rodhe, H., Sörlin, S., Snyder, P. K., Costanza, R., Svedin, U., … Foley, J. (2009). *Planetary Boundaries: Exploring the Safe Operating Space for Humanity*.

Sallée, J. B., Pellichero, V., Akhoudas, C., Vignes, L., & Schmidtko, S. (2021). Summertime increases in upper-ocean stratification and mixed-layer depth. *Nature*, *591*(7851), 592–598. https://doi.org/10.1038/s41586-021-03303-x

Shelford, E. J., & Suttle, C. A. (2018). Virus-mediated transfer of nitrogen from heterotrophic bacteria to phytoplankton. *Biogeosciences, 15*, 809–819. https://doi.org/10.5194/bg-15-809-2018.

Smith, K. L., Jr., Ruhl, H. A., Bett, B. J., & Kaufmann, R. S.(2009). Climate, carbon cycling, and deep-ocean ecosystems. *Proceedings of the National Academy of Sciences*, *106*(46), 19211-19218. https://doi.org/10.1073/pnas.0908322106

Spilling, K., Paul, A. J., Virkkala, N., Hastings, T., Lischka, S., Stuhr, A., Bermúdez, R., Czerny, J., Boxhammer, T., Schulz, K. G., Ludwig, A., & Riebesell, U. (2016). Ocean acidification decreases plankton respiration: Evidence from a mesocosm

experiment. *Biogeosciences, 13*(19), 4707–4719. https://doi.org/10.5194/bg-13-4707-2016

Steven W. Wilhelm, Curtis A. Suttle, Viruses and Nutrient Cycles in the Sea: Viruses play critical roles in the structure and function of aquatic food webs, *BioScience*, Volume 49, Issue 10, October 1999, Pages 781–788, https://doi.org/10.2307/1313569

Stockenreiter, M., Haupt, F., Seppälä, J., Tamminen, T., & Spilling, K. (2016). Nutrient uptake and lipid yield in diverse microalgal communities grown in wastewater. *Algal Research*, *15*, 77–82. https://doi.org/10.1016/j.algal.2016.02.013

Tiago, I., Chung, A. P., & Veríssimo, A. (2004). Bacterial diversity in a nonsaline alkaline environment: Heterotrophic aerobic populations. *Applied and Environmental Microbiology*, *70*(12), 7378–7387. https://doi.org/10.1128/AEM.70.12.7378-7387.2004

Subhas, A. V., Marx, L., Reynolds, S., Flohr, A., Mawji, E. W., Brown, P. J., & Cael, B. B. (2022). Microbial ecosystem responses to alkalinity enhancement in the North Atlantic Subtropical Gyre. *Frontiers in Climate, 4,* 784997. https://doi.org/10.3389/fclim.2022.784997

Sokal, R. R., and Rohlf, F. J. (eds.). (2013). *Biometry : The Principles and Practice of Statistics in Biological Research*. New York, NY: W. H. Freeman and Co.

Taucher, J., Bach, L. T., Boxhammer, T., Nauendorf, A., The Gran Canaria KOSMOS Consortium, Achterberg, E. P., Algueró-Muñiz, M., Arístegui, J., Czerny, J., Esposito, M., Guan, W., Haunost, M., Horn, H. G., Ludwig, A., Meyer, J., Spisla, C., Sswat, M., Stange, P., & Riebesell, U. (2017). Influence of ocean acidification and deep water upwelling on oligotrophic plankton communities in the subtropical North Atlantic: Insights from an *in situ* mesocosm study. *Frontiers in Marine Science, 4*. https://doi.org/10.3389/fmars.2017.00085

Tiago, I., Chung, A. P., & Veríssimo, A. (2004). Bacterial diversity in a nonsaline alkaline environment: Heterotrophic aerobic populations. *Applied and Environmental Microbiology*, *70*(12), 7378–7387. https://doi.org/10.1128/AEM.70.12.7378-7387.2004

Wilhelm, S. W., & Suttle, C. A. (1999). Viruses and nutrient cycles in the sea: Viruses play critical roles in the structure and function of aquatic food webs. *Bioscience, 49*(10), 781–788.

Welschmeyer, N. A. (1994). Fluorometric analysis of chlorophyll a in the presence of chlorophyll b and pheopigments. *Limnology and Oceanography*, *39*(8), 1985–1992. https://doi.org/10.4319/lo.1994.39.8.1985

Williamson, P., & Turley, C. (2012). Ocean acidification in a geoengineering context. In *Philosophical Transactions of the Royal Society A: Mathematical, Physical and Engineering Sciences*, *370, 1974, 4317–4342*. Royal Society. https://doi.org/10.1098/rsta.2012.0167

PREGUNTAS

Descripción detallada de las actividades desarrolladas durante la realización del TFT

El desarrollo del Trabajo de Fin de Título (TFT) se llevó a cabo mediante una serie de actividades organizadas en diferentes etapas, todas ellas esenciales para alcanzar los objetivos planteados. Inicialmente, se celebró una reunión con los tutores para definir los aspectos generales del proyecto. Durante esta sesión, se explicó la idea principal y los objetivos del estudio, que aún no estaban completamente delimitados debido a la naturaleza innovadora del tema. Esta fase implicó un enfoque exploratorio, ya que los resultados esperados no estaban claros y dependían en gran medida de los análisis que se realizarían a lo largo del trabajo.

La siguiente etapa consistió en trabajar con las bases de datos suministradas. Este proceso incluyó tareas como la organización, limpieza y estructuración de los datos, asegurándose de que estuvieran en un formato adecuado para el análisis. Posteriormente, se dedicó tiempo a la elaboración de gráficos y tablas que ayudaran a identificar patrones, tendencias y posibles anomalías en los datos, utilizando herramientas como Excel para una representación más clara.

Otra parte importante del trabajo fue la aplicación de análisis estadísticos, como el cálculo de valores p y otras pruebas que permitieron validar las relaciones entre las variables estudiadas. Los resultados obtenidos fueron representados mediante gráficos y tablas, los cuales facilitaron la interpretación y comunicación de los hallazgos en el informe final.

Finalmente, se integraron los resultados con estudios previos relevantes. Al tratarse de un tema poco explorado, esta etapa requirió una búsqueda exhaustiva de referencias que contextualizaran las observaciones y las conectaran con investigaciones anteriores. Este análisis permitió enmarcar los hallazgos en un contexto científico más amplio, aportando valor al proyecto.

En resumen, estas actividades permitieron no solo desarrollar el trabajo de manera efectiva, sino también mejorar competencias en análisis de datos, interpretación de resultados y uso de herramientas científicas.

Formación recibida (cursos, programas informáticos, etc.)

Aunque no se recibió una formación específica para el proyecto, los conocimientos adquiridos durante los estudios de grado y máster fueron fundamentales para enfrentar los desafíos planteados. Los tutores desempeñaron un papel importante al guiar y formar en aspectos especializados relacionados con la investigación desarrollada en este trabajo.

Durante el proceso, se adquirieron habilidades avanzadas en el manejo de herramientas como Excel, lo que facilitó la gestión y análisis de datos de manera más eficiente. Además, se aprendieron protocolos específicos y se aplicaron formatos académicos necesarios para la presentación de resultados en informes científicos.

En general, esta experiencia no solo permitió aplicar los conocimientos ya adquiridos, sino que también supuso un aprendizaje continuo en metodologías y técnicas que enriquecieron tanto la formación profesional como la académica.

Nivel de integración e implicación dentro del departamento y relaciones con el personal

La integración en el departamento fue limitada debido a las circunstancias particulares del máster, que combinaba una estructura compacta con la necesidad de compaginarlo

con un trabajo. Esto llevó a que gran parte del proyecto se desarrollara de manera remota, reduciendo las oportunidades de interacción directa con el equipo del departamento.

Sin embargo, se mantuvo una comunicación constante con los tutores, ajustándose a las necesidades del trabajo. En las fases más críticas, las interacciones eran frecuentes, mientras que en otras etapas el contacto era menos regular, dependiendo de los avances del proyecto. A pesar de la modalidad virtual predominante, la relación con los tutores fue fluida y efectiva, lo que facilitó el progreso del trabajo y la resolución de problemas.

Aspectos positivos y negativos más significativos relacionados con el desarrollo del TFT

Entre los aspectos positivos, destaca la oportunidad de trabajar en un tema innovador dentro de la oceanografía, lo que representó un reto y un estímulo intelectual. Esta experiencia permitió explorar una rama del conocimiento no abordada previamente, adquiriendo nuevas competencias y una visión más amplia sobre el campo de estudio.

Por otro lado, la novedad del tema también supuso una dificultad, ya que la limitada literatura disponible complicó la contextualización y comparación de los resultados obtenidos. Además, mi formación previa, centrada en la oceanografía física, no proporcionaba una base sólida en esta área específica, lo que se notó especialmente durante la interpretación de los datos. No obstante, estas dificultades impulsaron un esfuerzo adicional para superar los retos, resultando en un aprendizaje significativo y un crecimiento personal.

Valoración personal del aprendizaje conseguido a lo largo del TFT

Este trabajo fue una experiencia formativa muy enriquecedora. Permitió adquirir conocimientos sobre el efecto de la alcalinización oceánica mejorada en las bacterias heterotróficas, con un enfoque particular en nutrientes inorgánicos y orgánicos, DOC, DON, absorbancia y la dinámica de la materia orgánica disuelta. Se logró comprender mejor las interacciones entre estos elementos y su papel en los ciclos biogeoquímicos del océano.

A pesar de comenzar con una base limitada en este campo, el desarrollo del trabajo fortaleció habilidades analíticas y de interpretación de resultados. Este proceso no solo

enriqueció el conocimiento en áreas clave de la oceanografía, sino que también contribuyó significativamente al desarrollo profesional y académico en un tema de gran relevancia científica.